New Journal of Physics
The open access journal at the forefront of physics

Deutsche Physikalische Gesellschaft DPG IOP Institute of Physics

PAPER • OPEN ACCESS

Braiding of Majorana bound states in a driven-dissipative Majorana box setup

To cite this article: Kunmin Wu *et al* 2024 *New J. Phys.* **26** 123007

IOP Publishing New J. Phys. 26 (2024) 123007 https://doi.org/10.1088/1367-2630/ad96da

New Journal of Physics
The open access journal at the forefront of physics

Deutsche Physikalische Gesellschaft DPG
IOP Institute of Physics

Published in partnership with: Deutsche Physikalische Gesellschaft and the Institute of Physics

OPEN ACCESS

RECEIVED
9 October 2024

REVISED
18 November 2024

ACCEPTED FOR PUBLICATION
25 November 2024

PUBLISHED
6 December 2024

PAPER

Braiding of Majorana bound states in a driven-dissipative Majorana box setup

Kunmin Wu, Sadeq S Kadijani and Thomas L Schmidt*

Department of Physics and Materials Science, University of Luxembourg, 1511 Luxembourg, Luxembourg
* Author to whom any correspondence should be addressed.

E-mail: thomas.schmidt@uni.lu

Keywords: non-Abelian anyons, Majorana bound states, open quantum systems, topological quantum computation

Abstract

We investigate a system of Majorana box qubits, where each of the Coulomb blockaded boxes is driven by an applied AC voltage and is embedded in a dissipative environment. The AC voltage is applied between a pair of quantum dots, each of which is coupled by tunneling to a Majorana box qubit. Moreover, the dissipation is created by the coupling to an electromagnetic environment. Recent work has shown that in this case the Majorana bound states (MBSs) which form the computational basis can emerge as dark states, which are stabilized by the dissipation. In our work, we show that the same platform can be used to enable topological braiding of these dissipative MBSs. We show that coupling three such Majorana boxes allows a braiding transformation by changing the tunnel amplitudes adiabatically in time.

1. Introduction

Majorana bound states (MBSs) have been proposed to exist as zero-energy quasiparticles in several solid-state systems. Among the most promising experimental platforms are semiconductor nanowires with Rashba spin–orbit coupling in a magnetic field and subject to a superconducting proximity effect [1–14], chains of ferromagnetic atoms on top of a superconductor [15–31], or quantum spin Hall edge states coupled to superconductors [32–36]. The vibrant activity in this field is driven to a large extent by the intriguing properties of such MBSs, in particular their non-Abelian exchange statistics [37–44].

This nontrivial exchange statistics was first discussed in the context of two-dimensional p-wave superconductors, where vortices of the superconducting order parameter host MBSs [45–47]. Two such MBSs span a two-dimensional low-energy Hilbert space and a cyclic adiabatic transformation ('braiding') acting on the two MBSs can implement a topologically nontrivial, unitary transformation within this ground state subspace. The concept of braiding originally referred to an adiabatic exchange of the positions of two MBS, but other adiabatic processes, e.g. within the dark spaces of a dissipative open system as in this paper, can also give rise to non-Abelian topological transformations. In the experimental realizations mentioned above, MBS typically emerge at the ends of one-dimensional systems [48], but even in those cases adiabatic exchanges can often be implemented using, e.g. T-junctions [49], holonomic entangling [50–53] or changing superconducting fluxes [45, 54].

The non-Abelian statistics of MBSs are also the cornerstone of their proposed application in topological quantum computing [39, 55–57]. In that case, the Hilbert space spanned by the MBSs can be used to define a qubit state, and information in such a state would be stored nonlocally, rendering it robust to certain perturbations. Braiding them would allow the implementation of certain qubit gates.

So far, MBSs have mainly been considered in closed quantum systems. However, it was shown early on that open quantum systems can give rise to MBS as well [58–60] and that dissipation can help in the detection of MBSs [61–63]. An open quantum system is embedded in an environment and in the simplest case its reduced density matrix evolves according to the Lindblad equation [64–67]. While most quantum states decay in the presence of damping, certain dark states [68] of the Hilbert space may be immune to such dissipation [69–71]. In this case, damping can stabilize a dark state subspace which can contain MBSs

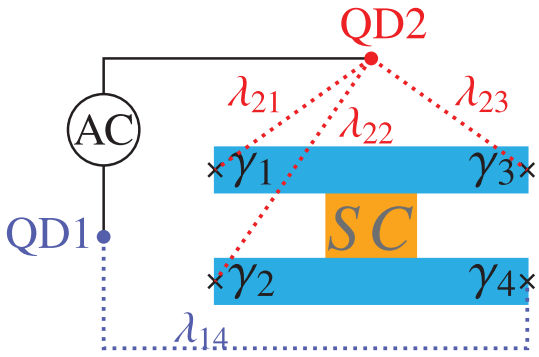

Figure 1. Two nanowires (blue rectangles) are connected by a superconducting (SC) bridge (orange rectangle). The four edge modes of these nanowires are Majorana bound states (MBSs) marked as γ_ν. These MBSs are tunnel coupled to the quantum dots QD1 and QD2, as indicated by the dashed lines, and $\lambda_{j\nu}$ denotes the tunneling amplitude from QD $d_j^\dagger$ to MBS γ_ν. An AC voltage is applied between the two QDs and drives the system.

[72–74]. This idea is behind the proposed realization of a Kitaev chain [48] in dissipative cold-atom systems [59].

The topological protection of MBSs rests on a conserved fermionic parity in the system. In that respect, MBSs emerging in quantum dots (QDs) [75] in the Coulomb blockade regime are beneficial because a large charging energy can protect them from charge fluctuations. Recently, it was shown that an open-system scenario can be created as well for MBSs in Majorana boxes coupled to tunneling junctions [76–78]. In this case, the Lindblad dynamics can in fact stabilize certain one-qubit and two-qubit Majorana states which are interesting for quantum computation [79, 80]. The proposed architecture combines the topological protection of MBSs with the robustness of driven-dissipative systems, and offers a high degree of tunability. This is why it might provide a new platform which harnesses the unavoidable damping processes present in all Majorana systems. However, in those previous works, it was not discussed how topological qubit operations could be performed on such driven-dissipative MBSs. Our paper fills this gap and will propose a braiding protocol which can be implemented in such a driven-dissipative Majorana system.

In our work, we will consider a setup consisting of Majorana boxes placed in a dissipative environment. To engineer dissipation, the Majorana boxes are linked via tunnel junctions to a driven fermionic reservoir, and damping is created by an electromagnetic Ohmic environment which affects tunneling [66, 67]. Depending on the chosen system parameters, this system can stabilize a dark state subspace of MBSs. We extend this setup to a network of three Majorana boxes. In this case, we show that an adiabatic periodic change of the system parameters can be used to drive the dark states and to implement a braiding operation on the MBS, which is manifested in a quantized topological winding number.

The structure of this article is as follows: in section 2, we briefly revisit the main results of [77] and show how a driven-dissipative Majorana box system can give rise to a dark state subspace. Next, in section 3, we start from the general Lindblad dynamics of a single Majorana box system and show how its dark states can be driven by changing the parameters, giving rise to quantized winding numbers. In section 4 we show how to implement such a braiding transformation in a system consisting of three Majorana boxes. Finally, we present our conclusions in section 5.

2. An open system with Majorana boxes

The basic building block of the system under study is shown in figure 1. A single Majorana box qubit consists of two Majorana nanowires, which can be realized using a superconductor-semiconductor heterostructure [10–14], such as InAs or InSb nanowires, coupled to a common floating superconductor. Its small size leads to a significant charging energy for the Majorana system. Moreover, each of the MBSs is coupled via tunneling to one of two QDs QD1 and QD2. An AC voltage between the two QDs can be used to pump electrons between them. Moreover, we assume that the whole system is embedded in an electromagnetic environment, which mainly affects the phases of the tunneling amplitudes between the QDs and the MBSs. The Hamiltonian and the approximations used are discussed in detail in [77], but we reiterate the essential steps to make our discussion self-contained.

We consider the resulting system as an open quantum system, where the electromagnetic field modes constitute a bosonic environment for the Majorana box. The system Hamiltonian consists of the Hamiltonian of the Majorana box ($H_{\rm box}$) and that of the QDs ($H_{\rm QD}$), as well as Hamiltonians for the (time-dependent) driving field between the QDs $H_{\rm drive}(t)$, the tunneling between the QDs and MBSs $H_{\rm tun}$, and the bosonic environment $H_{\rm env}$. The total Hamiltonian therefore reads,

$$H(t) \quad = H_{\rm box} + H_{\rm QD} + H_{\rm tun} + H_{\rm env} + H_{\rm drive}(t)\,. \tag{1}$$

At energies below the superconducting gap Δ_0, the MBSs γ_ν ($\nu \in \{1,\ldots,4\}$) and the Cooper pairs in the superconducting island are the only degrees of freedom of the Majorana box. The four MBSs span a four-dimensional Hilbert space. The Hamiltonian of the Majorana box is determined by its charging energy E_C and its total electron number $\hat{N}$, which comprises the Cooper pairs as well as the electrons in the MBSs,

$$H_{\rm box} = E_C\left(\hat{N} - N_g\right)^2. \tag{2}$$

We assumed that the direct overlaps between different MBSs are negligible. The parameter N_g accounts for the presence of a back-gate voltage which can be used to offset the charging energy and thus control the ground state of the box. When $N_g = 1$ the ground states have the fermion number $\hat{N} = 1$, and this condition is fulfilled for the two degenerate Majorana states with odd parity. The Majorana box will be trapped in this ground state subspace as long as the energy scale of any dynamics is lower than the charging energy E_C and the superconducting gap [77, 81, 82]. In the following, we will assume this to be the case, so we can drop the term $H_{\rm box}$ because it will merely act as a constant term in this reduced ground-state subspace.

The Majorana box is connected by tunneling to two QDs. We assume that each QD can be described by a single fermionic level,

$$H_{\rm QD} = \sum_{j=1}^{2} \epsilon_j d_j^\dagger d_j \tag{3}$$

with fermionic annihilation operators d_j. Each of the two QDs is coupled to one or more MBSs by electron tunneling,

$$H_{\rm tun} = t_0 e^{-i\hat{\phi}} \sum_{j\nu} e^{i\delta_j} \lambda_{j\nu} e^{-i\beta_{j\nu}} d_j^\dagger \gamma_\nu + \text{h.c.}, \tag{4}$$

where t_0 is the overall tunnel amplitude between QDs and the Majorana box. Moreover, $\hat{\phi}$ is a phase operator which obeys the commutator $[\hat{\phi}, \hat{N}] = -i$ and which is necessary to account for the change of electron number in the Majorana box upon tunneling. Moreover, the (dimensionless) tunable tunnel amplitudes between the QD electron d_j and MBS γ_ν are complex functions with real amplitudes $\lambda_{j\nu}$ and phases $\beta_{j\nu}$ in the interval $[0,\ \pi)$. Since the total electron number is fixed, we assume that the two QDs contain in total a single electron in order to allow for electron tunneling between the QDs.

The bath Hamiltonian $H_{\rm env}$ is a collection of harmonic oscillators b_m which constitute an Ohmic bath. Their main effects of the bath are to change the phases of the tunneling amplitudes between the QD and the MBSs,

$$\delta_j \quad = \textstyle\sum_m g_{jm}\left(b_m + b_m^\dagger\right), \tag{5}$$

with real-valued constants g_{jm}.

In the Coulomb valley regime, the charging term in $H_{\rm box}$ (2) pins the total charge $\hat{N}$ on the Majorana box to a fixed value. Therefore, the total occupation number of the two QDs also remains constant. As shown in figure 1, if the total occupation number of the QDs is even, this leads to a suppression of tunneling between the two QDs. Consequently, we will concentrate on cases with an *odd* total occupation number on the QDs in the following analysis, such that tunneling between QD1 and QD2 is possible.

2.1. Dynamics in the low-energy sector

Assuming tunneling to be weak, we can eliminate the tunneling term up to the second order in t_0 by using a Schrieffer–Wolff (SW) transformation. Before the SW transformation, the Hamiltonian can be written as a sum of an unperturbed term $H_0 = H_{\rm QD} + H_{\rm env} + H_{\rm drive}(t)$ and a small perturbation $H_{\rm tun}$. Then, the SW transformation is implemented using a unitary transformation e^S such that $H_{\rm eff} = e^S(H_0 + H_{\rm tun})e^{-S}$, where the generator S is of the order of the tunneling amplitude. By choosing S such that $H_{\rm tun} + [S, H_0] = 0$, the SW

transformation yields a transformed Hamiltonian $H_{\rm eff} \approx H_0 + [S, H_{\rm tun}]/2 = H_0 + H_{\rm cot}$, where terms of order t_0 have been eliminated. After the SW transformation, we thus obtain an effective cotunneling contribution,

$$\begin{aligned} H_{\rm cot} &= V_{\rm cot} + V_0, \\ V_{\rm cot} &= 2g_0 \left(e^{i\delta_{12}} A_{12} d_2^\dagger d_1 + \text{h.c.} \right), \\ V_0 &= g_0 \sum_{j=1,2} A_{jj} d_j^\dagger d_j, \end{aligned} \tag{6}$$

where $g_0 \equiv t_0^2/E_C$ and $\delta_{12} = \delta_2 - \delta_1$ with δ_j defined in equation (5). The operators A_{jk} account for the tunneling trajectories of the electrons through the Majorana boxes,

$$A_{jk} = \sum_{\mu<\nu} \left[\lambda_{j\nu} \lambda_{k\mu} e^{i\left(\beta_{k\mu} - \beta_{j\nu}\right)} - \lambda_{j\mu} \lambda_{k\nu} e^{i\left(\beta_{k\nu} - \beta_{j\mu}\right)} \right] \gamma_\mu \gamma_\nu. \tag{7}$$

Finally, we discuss the effect of the time-dependent drive. It is provided by an AC voltage with frequency ω_0 and amplitude $\mathcal{A}$ between the pair of QDs QD1 and QD2,

$$H_{\rm drive}(t) = 2\mathcal{A} \cos(\omega_0 t)\, d_1^\dagger d_2 + \text{h.c.} \tag{8}$$

When the AC frequency is close to the energy difference between two QDs, $\omega_0 \approx \epsilon_2 - \epsilon_1$, tunneling becomes resonant and it is possible to use the rotating wave approximation (RWA) [66, 68]. The RWA corresponds to going to a rotating frame and neglecting the fast oscillating terms proportional to $e^{\pm 2i\omega_0 t}$. In this case, the drive term takes the form,

$$H_{\rm drive}^{\rm RWA} = \mathcal{A} d_1^\dagger d_2 + \text{h.c.}. \tag{9}$$

Under the RWA, the amplitude $\mathcal{A}$ appears in the Lamb-shift Hamiltonian within the Lindblad equation that describes the dynamics of the QDs and the Majorana sector. When we trace out the degrees of freedom associated with the QDs, the amplitude $\mathcal{A}$ manifests indirectly through its effect on the occupation probability of the QDs. As a result, the total effective Hamiltonian now describes the MBSs and the quantum dot electrons, which are coupled to a bosonic bath via the term $V_{\rm cot}(t)$ in the cotunneling Hamiltonian (6),

$$H_{\rm eff} \quad = H_{\rm QD} + H_{\rm cot} + H_{\rm env} + H_{\rm drive}^{\rm RWA}. \tag{10}$$

This effective Hamiltonian is the starting point for describing the dynamics of the reduced system density matrix using a Lindblad master equation.

2.2. The Lindblad master equation for the MBSs

In the low-energy limit and using the other approximations explained in section 2.1, the coupling between the system and the environment is described by $H_{\rm cot}$, see equation (6). Next, we will use the Born-Markov approximation, in which we assume that the coupling to the bath is weak and that the bath relaxes fast to equilibrium. This approximation will give rise to a Master equation for the MBS system and QDs which will be of Lindblad form. The Lindblad equation maps the reduced system density matrix from its initial state to the steady state while ensuring that the basic properties of the density matrix remain fulfilled.

The reduced system state becomes factorized on a timescale that corresponds to the inverse of the dissipative gap of the reduced Lindbladian governing exclusively the Majorana sector. Hence, it is reasonable to approximate $\rho(t \to \infty)$ as $\rho_M(t \to \infty) \otimes \rho_{QD}$, where ρ_M and ρ_{QD} represent the reduced density matrices of the MBSs and QDs, respectively. After tracing over the environment and QD degrees of freedom, one obtains the Lindblad equation for the Majorana box [77],

$$\frac{d}{dt}\rho_M \quad = \mathcal{L}\rho_M(t) \approx \sum_{j\neq k=1}^{2} \Gamma_{jk} \left[A_{jk} \rho_M(t) A_{jk}^\dagger - \tfrac{1}{2} \left\{ A_{jk}^\dagger A_{jk}, \rho_M(t) \right\} \right], \tag{11}$$

where A_{jk} is the jump operator defined in equation (7), and Γ_{jk} is the corresponding transition rate, which is given by

$$\Gamma_{21} = 2\text{Re}[\Lambda_-], \; \Gamma_{12} = 2\text{Re}[\Lambda_+], \tag{12}$$

$$\Lambda_{\pm} = 4g_0^2 \int_0^{\infty} ds\, e^{\pm i\omega_0 s} \left\langle e^{\pm i[\delta_{12}(s)-\delta_{12}(0)]} \right\rangle_{\text{env}}$$
$$= 4g_0^2 \int_0^{\infty} ds\, e^{\pm i\omega_0 s}\, e^{J_{\text{env}}(s)}, \tag{13}$$

where the correlation function of the bosonic bath at temperature T is,

$$J_{\text{env}}(t) = \int \frac{d\omega}{\pi} \frac{\mathcal{J}(\omega)}{\omega^2} \left[\coth\left(\frac{\omega}{2T}\right) (\cos(\omega t) - 1) - i \sin(\omega t) \right]. \tag{14}$$

We assume the bath to be Ohmic, so the spectral density $\mathcal{J}(\omega)$ is proportional to the bath frequency ω for frequencies up to a cut-off frequency ω_c [67].

From the bath correlation function (14), one can prove that $J_{\text{env}}(-t - i/T) = J_{\text{env}}(t)$, which leads to $\Lambda_- = e^{-\omega_0/T}\Lambda_+$. Therefore, the forward and backward transition rates are related as,

$$\Gamma_{21} = e^{-\omega_0/T}\Gamma_{12}, \tag{15}$$

leading to a suppression of Γ_{21} with respect to Γ_{12}.

In the Lindblad equation (11), we neglected the unitary time evolution $-i[H_{LS}, \rho_M]$ with the 'Lamb shift' Hamiltonian $H_{LS} = \sum_{j,k} h_{jk} A_{jk}^{\dagger} A_{jk}$. The prefactor h_{jk} is the imaginary part of $\Lambda_{\pm}$ (13). In the steady state, the system is in a mixed state composed of dark states, each of which is annihilated by A_{jk}. Hence, the unitary dynamics due to H_{LS} vanishes in the steady state and does not influence the dark-state subspace where braiding will be implemented.

In contrast, if the two MBS have a nonzero overlap, the unitary part of the time evolution will affect the steady state. The overlap Hamiltonian is given by $H_{\text{overlap}} = \sum_{\nu>\mu} i\epsilon_{\nu\mu}\gamma_\nu\gamma_\mu$, where $\epsilon_{\nu\mu}$ represents the hybridization energy between the MBSs γ_ν and γ_μ. Importantly, the Hamiltonian H_{overlap} does not necessarily commute with the steady state. As a result, the unitary time evolution governed by H_{overlap} causes the system state to oscillate between the dark states on a timescale determined by the hybridization energies $\epsilon_{\nu\mu}$. Oscillations like these are problematic for quantum gates because they introduce time-dependent phase shifts, which can interfere with braiding operations. Thus, it is important to ensure that braiding occurs faster than this oscillation timescale, determined by the inverse hybridization energies, but remains slow compared to the inverse superconducting gap. Since this constraint is common to all braiding protocols [41], we do not pursue it further here.

One potential experimental platform for realizing the proposed system is an InSb/NbTiN heterostructure, where the InSb wire can be several micrometers long with diameters on the order of tens of nanometers [10]. In this configuration, the charging energy E_C typically has a magnitude of about 1 meV and the superconducting gap Δ_0 is on the order of 1 meV when the temperature T is below 15 K [10]. It is important to ensure that the other parameters are much smaller than both the charging energy and the superconducting gap. In [77], a numerical analysis indicates that the stabilization timescales are on the order of a few nanoseconds when the parameters are set as $E_C = 1\,\text{meV} = 400g_0$, $T = 4g_0$, $\omega_0 = 40g_0$, $\omega_c = 200g_0$, and $\mathcal{A} = 0.1g_0$.

So far, we have reviewed the dissipative dynamics of the Majorana box within the Born-Markov approximation. The ensuing discussion rests on the fact that the steady-state density matrices which obey $\mathcal{L}\rho_M(t \to \infty) = 0$ form a dark state subspace, which allows the stabilization of certain Majorana qubit states.

3. Topological phases in open Majorana boxes

In this section, we consider a general expression for the steady state density matrix in the open system consisting of a single Majorana box coupled to two QDs. The dissipation in this system is described by the Lindblad equation (11) when the correlation time of the system is much longer than that of the bath. Then, we follow [59] to show in which cases there is topological order in the steady state. In the end, we provide a stabilization protocol which drives the system in figure 1 to a pure state with topological order.

3.1. General form of steady-state density matrix

We will first explain how a topological transformation can be implemented within the dark state subspace, as generated by the steady-state solutions of the Lindblad equation (11). That equation holds for a single Majorana box and the associated two-dimensional dark state subspace for a given fermionic parity. Non-Abelian braiding is impossible in a two-dimensional Hilbert space because the braid matrix can always

be diagonalized, resulting only in (Abelian) exchange phases. Nevertheless, we present the ensuing discussion to explain in a compact form how braiding will be implemented later in a larger Majorana box qubit system.

To keep this discussion general, we consider a Lindblad equation of the form (11) for a density matrix $\rho(t)$ but with an arbitrary 2×2 jump operator K and a general damping amplitude Γ,

$$\frac{d}{dt}\rho(t) \quad = \mathcal{L}[K]\rho(t) = \Gamma\left[K\rho(t)K^\dagger - \tfrac{1}{2}\left\{K^\dagger K, \rho(t)\right\}\right]. \tag{16}$$

From the relation between the two transition rates in equation (15), one finds that the rate Γ_{21} is exponentially suppressed for $T \ll \omega_0$ in the low-energy regime. Thus, we only consider the trajectories from QD 1 to QD 2. The jump operator and the density matrix can be parametrized as follows,

$$K = \boldsymbol{k}\cdot\boldsymbol{\sigma}, \tag{17}$$

$$\rho(t) = \frac{1}{2}\left(\sigma_0 + \boldsymbol{n}(t)\cdot\boldsymbol{\sigma}\right), \tag{18}$$

with $\boldsymbol{k} = (k_x e^{i\phi_x}, k_y e^{i\phi_y}, k_z e^{i\phi_z})$ and $\boldsymbol{n} = (n_x, n_y, n_z)$, where $k_{x,y,z}\in\mathbb{R}$, $n_{x,y,z}\in\mathbb{R}$ and $\phi_{x,y,z}\in[0,\pi)$. Moreover, σ_0 denotes the identity matrix and $\boldsymbol{\sigma}$ is the vector of Pauli matrices. As the product of two Pauli matrices satisfies $\sigma_j\sigma_k = \delta_{jk}\sigma_0 + i\epsilon_{jkl}\sigma_l$ with the Levi-Civita symbol ϵ_{jkl} one finds $(\boldsymbol{\nu}_1\cdot\boldsymbol{\sigma})(\boldsymbol{\nu}_2\cdot\boldsymbol{\sigma}) = (\boldsymbol{\nu}_1\cdot\boldsymbol{\nu}_2)\sigma_0 + i\boldsymbol{\sigma}\cdot(\boldsymbol{\nu}_1\times\boldsymbol{\nu}_2)$ for two arbitrary 3D vectors $\boldsymbol{\nu}_1$ and $\boldsymbol{\nu}_2$. This makes it possible to rewrite equation (16) as,

$$\mathcal{L}[K]\rho(t) \quad = \tfrac{\Gamma}{2}\boldsymbol{\sigma}\cdot\left[2i\boldsymbol{k}\times\boldsymbol{k}^* + (\boldsymbol{k}\cdot\boldsymbol{n}(t))\boldsymbol{k}^* + (\boldsymbol{k}^*\cdot\boldsymbol{n}(t))\boldsymbol{k} - 2|\boldsymbol{k}|^2\boldsymbol{n}(t)\right]. \tag{19}$$

As the steady state ρ_s should satisfy $d\rho_s/dt = \mathcal{L}[K]\rho_s = 0$, we can use equation (19) to express the corresponding steady-state Bloch vector $\boldsymbol{n}_s$ in terms of the components of the vector $\boldsymbol{k}$,

$$\boldsymbol{n}_s = -\tfrac{2}{|\boldsymbol{k}|^2}\left(k_y k_z \sin\left(\phi_{yz}\right),\ k_z k_x \sin\left(\phi_{zx}\right),\ k_x k_y \sin\left(\phi_{xy}\right)\right), \tag{20}$$

with $\phi_{jk} = \phi_j - \phi_k$. Next we need to determine how to ensure the existence of a chiral symmetry, which induces a topological order in the steady state.

3.2. Topological order of the steady-state density matrix

For quantum computation, the steady state should ideally be pure, i.e. $\rho_s^2 \equiv \rho_s$. According to equation (18), this corresponds to $\boldsymbol{n}_s$ being a unit vector. A sufficient condition for the steady-state Bloch vector (20) to have unit length is,

$$k_y^2 = -k_x^2 e^{\pm 2i\left(\phi_y-\phi_x\right)} - k_z^2 e^{\pm 2i\left(\phi_y-\phi_z\right)}. \tag{21}$$

As the values of k_x, k_y, and k_z must be real, only discrete values are allowed for the differences of the phases ϕ_j. Since in an adiabatic transformation it should be possible to vary the parameters along a continuous path, we choose the phases of the vector $\boldsymbol{k}$ as follows,

$$\phi_x - \phi_y = \frac{\pi}{2}, \qquad \phi_z - \phi_y = \frac{\pi}{2}. \tag{22}$$

These conditions lead to the following vector $\boldsymbol{k}$ and the corresponding steady-state Bloch vector $\boldsymbol{n}_s$,

$$\boldsymbol{k} = \left(ik_x, \operatorname{sgn}\left(k_y\right)\sqrt{k_x^2+k_z^2}, ik_z\right)e^{i\phi_y}, \tag{23}$$

$$\boldsymbol{n}_s = \left(\tfrac{k_z}{k_y}, 0, -\tfrac{k_x}{k_y}\right). \tag{24}$$

One should note that there is still one free phase ϕ_y in the vector $\boldsymbol{k}$, but this does not affect the Bloch vector $\boldsymbol{n}_s$.

The steady state being pure is one of the conditions for rotations of the qubit state to give rise to a topological phase. The second condition is the existence of a chiral symmetry [59]. This latter exists if it is possible to find a unitary symmetry operator Σ such that,

$$\Sigma(\boldsymbol{n}\cdot\boldsymbol{\sigma})\Sigma^\dagger = -(\boldsymbol{n}\cdot\boldsymbol{\sigma}) \ \Leftrightarrow\ \{\Sigma,\ \boldsymbol{n}\cdot\boldsymbol{\sigma}\} = 0. \tag{25}$$

Writing $\Sigma = \boldsymbol{a}\cdot\boldsymbol{\sigma}$ with a unit vector $\boldsymbol{a}$, equation (25) is equivalent to the Bloch vector $\boldsymbol{n}$ and the vector $\boldsymbol{a}$ being orthogonal, i.e. $\boldsymbol{a}\cdot\boldsymbol{n} = 0$. Hence, the Bloch vector can only rotate on the Bloch sphere in a plane with

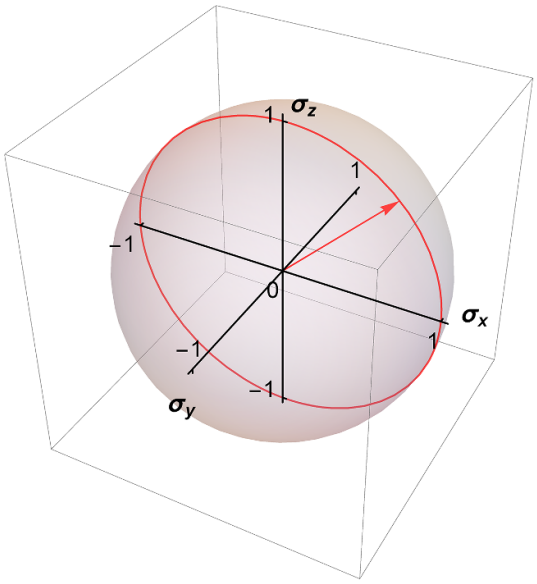

Figure 2. The Bloch vector (24) of a pure state is the red arrow in the Bloch sphere. While we rotate the qubits by changing parameters adiabatically, this Bloch vector also winds around the red solid unit circle in the $\sigma_x - \sigma_z$ plane.

normal vector $\boldsymbol{a}$. For the family of Bloch vectors in equation (24), the chiral symmetry operator is given by the pure-state Bloch vector $\boldsymbol{a} = (0,1,0)$ because $\boldsymbol{n}$ lies in the y plane (see figure 2).

As a consequence, adiabatically rotating the Bloch vector (24) between time $t = t_0$ and time $t = t_f$ along the circle shown in figure 2 spans the solid angle,

$$\Omega = \int_{t_0}^{t_f} dt\,[\boldsymbol{n}(k_x,k_z) \times \partial_t \boldsymbol{n}(k_x,k_z)] \cdot \boldsymbol{a} \tag{26}$$

$$= \int_{t_0}^{t_f} dt\,\frac{k_x \partial_t k_z - k_z \partial_t k_x}{k_z^2 + k_x^2}. \tag{27}$$

By writing n_x and n_z in polar coordinates as $n_x(t) = \sin\Theta(t)$ and $n_z(t) = \cos\Theta(t)$, we encode the adiabatic time evolution into the angle $\Theta(t)$. Then, the solid angle becomes (see also appendix A) ,

$$\Omega = \int_{t_0}^{t_f} dt\,\partial_t \Theta(t) = \Theta(t_f) - \Theta(t_0). \tag{28}$$

As $\Theta = \arctan(n_x/n_z) = -\arctan(k_z/k_x)$, we conclude that the solid angle only depends on the initial and final positions of the Bloch vector.

Hence, a cyclic adiabatic change of parameters leads to a winding number $\Omega = 2\pi n$ with $n \in \mathbb{Z}$. It is topological in that it is quantized and independent of the exact time-dependent function chosen for the adiabatic change of parameters. The next step is to determine the winding number explicitly for the driven-dissipative Majorana system.

3.3. The physical tunneling system for a single Majorana box

We now consider the tunneling couplings as shown in figure 1. Taking into account all possible transport processes from QD1 to QD2, we can deduce the following jump operator using equation (7),

$$K_{12} = \left(k_x e^{i\phi_x}, k_y e^{i\phi_y}, k_z e^{i\phi_z}\right) \cdot \boldsymbol{\sigma}, \tag{29}$$

where

$$k_x e^{i\phi_x} = \lambda_{14}\lambda_{22} e^{-i\beta_{14}+i\beta_{22}-i\pi/2}, \tag{30}$$

$$k_y e^{i\phi_y} = \lambda_{14}\lambda_{21} e^{-i\beta_{14}+i\beta_{21}-i\pi/2}, \tag{31}$$

$$k_z e^{i\phi_z} = \lambda_{14}\lambda_{23} e^{-i\beta_{14}+i\beta_{23}-i\pi/2}. \tag{32}$$

The steady-state Bloch vector should be of the form (20). To stabilize such a pure state, the tunneling parameters should fulfill the conditions in equations (21) and (22), which lead to

$$\beta_{22} = \beta_{23} = \beta_{21} + \tfrac{\pi}{2}, \qquad \lambda_{21}^2 = \lambda_{22}^2 + \lambda_{23}^2. \tag{33}$$

In this case, we obtain the following results for the vector $\boldsymbol{k}$ and the pure-state Bloch vector $\boldsymbol{n}_s$,

$$\boldsymbol{k} = \left(i\lambda_{22}, \mathrm{sgn}\,(\lambda_{21})\sqrt{\lambda_{22}^2+\lambda_{23}^2}, i\lambda_{23}\right)\lambda_{14}e^{i\Phi_y}, \tag{34}$$

$$\boldsymbol{n}_s = \frac{\mathrm{sgn}(\lambda_{21})}{\sqrt{\lambda_{23}^2+\lambda_{22}^2}}\left(\lambda_{23}, 0, -\lambda_{22}\right), \tag{35}$$

where $\Phi_y = \beta_{21} - \beta_{14} - \pi/2$.

If we consider again a time-periodic adiabatic change of the parameters $\lambda_{22}(t)$ and $\lambda_{23}(t)$, we can introduce polar coordinates such that their time-dependence is indicated by the azimuthal angle φ,

$$\lambda_{22}(t) = -r\cos\varphi(t), \qquad \lambda_{23} = r\sin\varphi(t). \tag{36}$$

The steady-state Bloch vector (35) thus evolves in time as $\boldsymbol{n}_s(t) = \mathrm{sgn}(\lambda_{21})(\sin\varphi(t), 0, \cos\varphi(t))$. Inserting this Bloch vector into equation (28) gives the quantized solid angle of $\Omega = 2\pi$ for a single loop in parameter space.

3.4. Summary

We began this section by considering a general expression for the steady-state Bloch vector (20) of a Majorana box coupled to two QDs, focusing on the scenario where one transition rate is dominant. To drive the system to a pure steady state, we can choose a parameter set satisfying the condition (22). This choice leads to the existence of a chiral symmetry (25) in the steady state, so rotating the Bloch vector (24) on the Bloch sphere can yield a quantized winding number. It is given by the solid angle (27) spanned during the time evolution of the Bloch vector. The realization of the topological order in this reduced parameter space arises from the fact that the winding number is quantized and does not depend on the trajectory of the parameters over time.

We showed how a topological phase can arise from adiabatic changes in the parameters of a driven-dissipative Majorana box qubit. However, the requirement that the stabilized dark state should be a pure state constrains the parameter ranges for the allowed tunnel couplings. In addition, the parameter space needs to allow for the definition of a chiral symmetry operator. The reduced parameter space leaves sufficient degrees of freedom to allow an adiabatic rotation of the qubit state vector which gives rise to a topological winding number.

For braiding, however, we will need multiple dark states in the same parity subspace, whereas the dark state subspace of a single Majorana box has at most two dark states of a given parity. Therefore, in the subsequent section, we will consider the stabilization and rotation of a qubit state in a system consisting of more than one coupled Majorana box and develop a braiding protocol for that system.

4. Braiding in the decoherence-free subspace by adiabatic parameter changes

A braiding process in this driven-dissipative system can be realized by transitioning the steady state from one dark state to another one in the same parity subspace, while the system parameters are varied adiabatically along a closed path. The following requirements should be fulfilled to allow such braiding:

(i) The dark state subspace should contain multiple dark states with the same parity.
(ii) The dark states should be parameter-dependent so that they can be reached by adiabatically changing parameters.
(iii) Dark states do not disappear and do not cross when parameters are slowly tuned during braiding.

In the Lindblad equation $\dot{\rho} = \mathcal{L}[K]\rho$, a dark state can be found as the eigenstate of the jump operator with eigenvalue zero [60]. If a state $|\psi\rangle$ satisfies $K|\psi\rangle = 0$, this implies that $\mathcal{L}[K]|\psi\rangle\langle\psi| = 0$, so that $\rho = |\psi\rangle\langle\psi|$ is the pure steady state of the system. In this section, we begin by considering an ideal jump operator whose dark states can fulfill the above three requirements. Next, we propose a geometry of tunneling couplings which realizes this jump operator and uses it to derive a braiding protocol.

4.1. The ideal jump operator

In a braiding transformation, an adiabatic change of system parameters along a closed path in parameter space brings the system from an initial state ρ_i to a final state $\rho_f = U\rho_i$, where U is the braiding matrix. If we prepare an initial state with a given parity and use a jump operator which does not couple different parity sectors, the two parity blocks in the density matrix will remain separated during the braiding protocol, i.e. $\mathcal{L}[K]\rho = \mathcal{L}[K_{\text{even}}]\rho_{\text{even}} \oplus \mathcal{L}[K_{\text{odd}}]\rho_{\text{odd}}$. Since the two parity sectors are uncoupled, we will consider only the odd parity sector for the rest of this section.

As described in the first requirement, we need at least two Majorana qubits to obtain two dark states with the same parity. In this case, the jump operator K_{odd} for two coupled Majorana boxes is represented as a 2×2 matrix within the odd-parity subspace spanned by the states $\{|01\rangle, |10\rangle\}$. For a general 2×2 jump operator, we can use the expression in equation (29). Its eigenvalues and the corresponding eigenstates are

$$K_{\text{odd}}\,|k_\pm\rangle = \pm|\boldsymbol{k}|\,|k_\pm\rangle, \tag{37}$$

with $|k_\pm\rangle = (k_z e^{i\phi_z} \pm |\boldsymbol{k}|,\ k_x e^{i\phi_x} + k_y e^{i\phi_y})$. A nonzero K_{odd} has a single dark state $(k_z e^{i\phi_z}, k_x e^{i\phi_x} + k_y e^{i\phi_y})$. Therefore, this setup does not provide sufficient ingredients for braiding, namely *multiple* parameter-dependent dark states in the same-parity subspace. Therefore, we need to extend the Hilbert space by adding one more Majorana box.

In the case of coupled three Majorana boxes, the odd-parity subspace is four-dimensional, so we assume that K_{odd} is a 4×4 matrix in the odd-parity state manifold spanned by $\{|001\rangle, |010\rangle, |100\rangle, |111\rangle\}$. A possible choice for the jump operator, which will turn out to be realizable in the Majorana box system, is

$$K_{\text{odd}} = \begin{pmatrix} 0 & f_1 & -ff_1 & 0 \\ g_1 & 0 & 0 & gg_1 \\ g_2 & 0 & 0 & gg_2 \\ 0 & f_2 & -ff_2 & 0 \end{pmatrix}, \tag{38}$$

where f and g are real functions of the tunnel couplings, $f(\lambda_{jv}, \beta_{jv})$ and $g(\lambda_{jv}, \beta_{jv})$, such that the adiabatic time evolution is encoded in f and g. This jump operator gives rise to the two dark states, $K_{\text{odd}}\,|\psi_{1,2}\rangle = 0$, with

$$|\psi_1\rangle = N_1\,(-g|001\rangle + |111\rangle)\,, \tag{39}$$

$$|\psi_2\rangle = N_2\,(f|010\rangle + |100\rangle)\,, \tag{40}$$

where N_1 and N_2 are normalization constants. These two dark states are independent of $f_{1,2}$ and $g_{1,2}$, yet they are distinct when one of g_1 or g_2 is non-zero, and simultaneously, one of f_1 or f_2 is non-zero. Moreover, they depend on the tunneling parameters through f and g, which are required for braiding in the dark state subspace. They do not coalesce for any combinations of f and g.

The other two eigenvalues of K_{odd} and their corresponding eigenvectors are, respectively,

$$K_{\text{odd}}\,|\psi_\pm\rangle = \pm\sqrt{(f_1 + f_2 g)\,(g_1 - f g_2)}\,|\psi_\pm\rangle, \tag{41}$$

$$|\psi_\pm\rangle = N_3 \begin{pmatrix} f_1\sqrt{g_1 - f g_2} \\ \pm g_1\sqrt{f_1 + f_2 g} \\ \pm g_2\sqrt{f_1 + f_2 g} \\ f_2\sqrt{g_1 - f g_2} \end{pmatrix} \tag{42}$$

with a normalization N_3. Since the eigenvalues (41) also depend on the parameters f and g, it is possible that they become zero when $f_1 = -f_2 g$ or $g_1 = f g_2$ during the adiabatic change in parameters. In that case, the eigenvectors $|\psi_\pm\rangle$ will coalesce with one of the dark states, but this does not affect the braiding protocol because the two dark states still remain distinct.

Hence, the jump operator (38) constitutes a viable option for braiding, and the next step is to realize this operator in the Lindblad equation (11), such that the steady state will be given by the two dark states $|\psi_1\rangle$ and $|\psi_2\rangle$.

4.2. The pure steady state and its topological order

We start again from the Lindblad equation (11) and consider the weak driving regime as in section 3.1. In this case $\Gamma_{12} \gg \Gamma_{21}$, so we focus on Γ_{12} as the dominant decay rate. The Lindblad term $\mathcal{L}[K_{\text{odd}}]$ with the jump operator (38) then drives the Majorana qubits to a steady state ρ_s obeying $\mathcal{L}[K_{\text{odd}}]\rho_s = 0$.

As we show in appendix B, we can use the following ansatz for the steady state density matrix,

$$\rho_s = \sum_{n=0}^{3} a_{nn}|n\rangle\langle n| + \sum_{n>m}\left[(a_{nm}+ib_{nm})\,|n\rangle\langle m| + \text{h.c.}\right], \tag{43}$$

where $a_{nm}, b_{nm} \in \mathbb{R}$ and the states $|0\rangle$, $|1\rangle$, $|2\rangle$ and $|3\rangle$ are shortcuts for the odd-parity states $|001\rangle$, $|010\rangle$, $|100\rangle$ and $|111\rangle$, respectively. Due to the properties of a density matrix, $a_{nn} \geqslant 0$ and $\sum_n a_{nn} \equiv 1$ for all n. Using the basis vectors $|\psi_1\rangle$ and $|\psi_2\rangle$ from equations (39) and (40) as well as two orthonormal vectors $|\psi_3\rangle$ and $|\psi_4\rangle$,

$$|\psi_3\rangle = \tfrac{1}{\sqrt{1+g^2}}\left(|001\rangle + g|111\rangle\right), \tag{44}$$

$$|\psi_4\rangle = \tfrac{1}{\sqrt{1+f^2}}\left(-|010\rangle + f|100\rangle\right), \tag{45}$$

one finds that the pure steady state ρ_s can be constructed from the dark states $|\psi_1\rangle$ and $|\psi_2\rangle$ as follows,

$$\rho_s = \left(\sqrt{1-F^2}e^{i\alpha_1}|\psi_1\rangle + Fe^{i\alpha_2}|\psi_2\rangle\right) \otimes \text{h.c.}, \tag{46}$$

where the following two conditions have to be satisfied (see equation (B.5) in appendix B),

$$f^2 = \frac{1+f^2}{f}a_{12} \text{ and } f^2 = 1 + \frac{1+g^2}{g}a_{03}, \tag{47}$$

and where a_{12} and a_{03} are the real parts of the elements at $|010\rangle\langle 101|$ and $|001\rangle\langle 110|$ in the general form of the steady state (43), respectively. Moreover, the phases α_1 and α_2 are associated to the argument of the element at $|100\rangle\langle 110|$ by $\arctan(b_{23}/a_{23}) = \alpha_1 - \alpha_2$.

The same result can also be proven by writing the Liouvillian superoperator $\mathcal{L}$ in the form of a matrix [77]. After some algebra, one can find four dark states corresponding to the vectorized forms of $|\psi_l\rangle\langle\psi_m|$, with $l, m \in \{1,2\}$. The other eigenstates have negative eigenvalues, such that they decay exponentially over time. The nearest non-zero eigenvalue is referred to as the dissipative gap. The transition of the Majorana sector towards dark states occurs over a timescale determined by the inverse of this dissipative gap.

To ensure the chiral symmetry required for the existence of a topological phase, we focus on linear combinations of two dark states with equal phases, $\alpha_1 = \alpha_2$, and obtain the following density matrix from equation (46) (see also appendix B),

$$\rho_s = \left(1-F^2\right)|\psi_1\rangle\langle\psi_1| + F^2|\psi_2\rangle\langle\psi_2| + F\sqrt{1-F^2}\left(|\psi_1\rangle\langle\psi_2| + |\psi_2\rangle\langle\psi_1|\right). \tag{48}$$

Considering this density matrix as a vector on the Bloch sphere spanned by $\{|\psi_1\rangle, |\psi_2\rangle\}$, we can again write $\rho_s = (\sigma_0 + \boldsymbol{n}\cdot\boldsymbol{\sigma})/2$ with

$$\boldsymbol{n} = \left(2F\sqrt{1-f^2}, 0, 1-2f^2\right). \tag{49}$$

The chiral symmetry is again implemented by $\Sigma = \sigma_y$, and upon an adiabatic change of parameters, the Bloch vector (49) rotates in the σ_x-σ_z plane. This is analogous to figure 2, but the Pauli matrices here are in the space of dark states $\{|\psi_1\rangle, |\psi_2\rangle\}$.

As in section 3.2 the solid angle Ω is given by the winding number of the Bloch vector (49) between time t_0 to t_f (see appendix A),

$$\begin{aligned}\Omega &= \Theta\left[f(t_f), g(t_f)\right] - \Theta\left[f(t_0), g(t_0)\right], \\ \Theta &= \arctan\left(\frac{n_x}{n_z}\right) = \arctan\left(\frac{2F\sqrt{1-F^2}}{1-2F^2}\right)\end{aligned} \tag{50}$$

The tunnel couplings are encoded in the functions f and g, whose periodic change can be expressed using polar coordinates with an angle $\theta(t_f) = \theta(t_0) + 2\pi$,

$$f(t) = r\cos\left[\theta(t)\right] \text{ and } g(t) = r\sin\left[\theta(t)\right]. \tag{51}$$

For a nontrivial braiding process, the Bloch vector (49) should wind about a semicircle while the parameters are driven along a closed loop back to their initial values. We therefore choose the function $F(f,g) \in [-1,1]$ as follows,

$$F\left[\theta(t)\right] = \sin\left[\frac{\theta(t)}{4}\right] = \sin\left[\frac{1}{4}\arcsin\left(\frac{g}{\sqrt{f^2+g^2}}\right)\right]. \tag{52}$$

In this case, the Bloch vector (49) becomes $\boldsymbol{n} = (\sin(\theta/2), 0, \cos(\theta/2))$ and the solid angle (50) reaches $\Omega = \pi$ after driving f and g for one period,

$$\begin{aligned} \theta(t_0) &= 0, \quad \boldsymbol{n}(t = t_0) = (0,0,1), \\ \theta(t_f) &= 2\pi, \quad \boldsymbol{n}(t = t_f) = (0,0,-1). \end{aligned} \tag{53}$$

The corresponding braiding operation can be expressed as a braiding operator $B = \sigma_y$ acting on the Hilbert space spanned by the two dark states (39) and (40),

$$B[\boldsymbol{n}(t = t_0) \cdot \boldsymbol{\sigma}] B^\dagger = \boldsymbol{n}(t = t_f) \cdot \boldsymbol{\sigma} \Rightarrow B\sigma_z B^\dagger = -\sigma_z. \tag{54}$$

With the ideal jump operator K_{odd} in equation (38), the Majorana qubits are stabilized in the dark state subspace where we can carry out braiding in the odd-parity subspace by tuning the tunneling parameters. To achieve this, it is necessary to prepare an odd-parity initial state of the system and the phase coherence between two dark states should ensure the chiral symmetry in the steady state (48) (see appendix B. The next step is to find a tunneling system whose jump operator provides the structure of K_{odd} in equation (38), and then demonstrate a braiding protocol in this open system.

4.3. The tunneling system and the braiding protocol

In this section, we consider the same open quantum system as depicted in figure 1, but with the inclusion of two additional Majorana boxes. Analogously to equation (1), the total Hamiltonian is

$$H(t) = H_{\text{box}} + H_{\text{QD}} + H_{\text{env}} + H_{\text{drive}}(t) + H_{\text{tun,e}} + H_{\text{tun},\gamma}, \tag{55}$$

where H_{box}, H_{QD}, H_{env}, and $H_{\text{drive}}(t)$ represent the Hamiltonian of the Majorana box, QDs, environment, and the time-dependent driving field, respectively. For three Majorana boxes, $H_{\text{box}} = E_C \sum_{n=1}^{3} (\hat{N}_n - N_g)^2$. The tunneling Hamiltonian consists of two contributions. Electron tunneling between the QDs and Majorana box n is represented by

$$H_{\text{tun,e}} = t_0 \sum_{n=1}^{3} \sum_{j=1}^{2} \sum_{\mu=1}^{4} \lambda_{j,n\mu} e^{-i\beta_{j,n\mu}} e^{-i\hat{\phi}_n + i\delta_j} d_j^\dagger \gamma_{n\mu} + \text{h.c.}, \tag{56}$$

while direct tunneling between the two Majorana boxes (the box n and the box n') is described by

$$H_{\text{tun},\gamma} = E_C \sum_{n \neq n'=1}^{3} \sum_{\mu,\nu=1}^{4} i\tilde{t}_{nn'} \gamma_{n\mu} \gamma_{n'\nu}, \tag{57}$$

with the dimensionless parameter $\tilde{t}_{nn'} = t_{nn'}/E_C$, and $t_{nn'}$ is the tunnel coupling energy between the boxes n and n'. Here, we assume that $t_{nn} = 0$ and $t_{nn'} > 0$ for all amplitudes.

In analogy to section 2.1, we apply the RWA and the SW transformation (see appendix C). In the SW transformation, the small perturbations are the couplings between QDs and MBSs t_0 as well as those between the Majorana boxes $t_{nn'}$. For three coupled Majorana boxes, the SW transformation should be expanded up to the fourth order to obtain the cotunneling Hamiltonian in the low-energy regime. For large E_C, the result can be approximated as

$$H_{\text{cot}} \approx \sum_{r=2}^{4} H_{\text{cot}}^{(r)} = \sum_{r=2}^{4} \left(\frac{1}{(r-1)!} - \frac{1}{r!} \right) \left(\frac{2}{E_C} \right)^{r-1} (H_{\text{tun}})^r, \tag{58}$$

where $H_{\text{tun}} = H_{\text{tun,e}} + H_{\text{tun},\gamma}$.

In this cotunneling Hamiltonian, we only retain terms describing complete tunneling trajectories between two dots because the remaining terms would only result in subleading corrections to higher-order tunneling processes. Hence, we find

$$H_{\text{cot}}^{(2)} \approx \frac{1}{E_C} H_{\text{tun,e}} H_{\text{tun,e}}, \tag{59}$$

$$H_{\text{cot}}^{(3)} \approx \frac{4}{3E_C^2} H_{\text{tun,e}} H_{\text{tun},\gamma} H_{\text{tun,e}}, \tag{60}$$

$$H_{\text{cot}}^{(4)} \approx \frac{1}{E_C^3} H_{\text{tun,e}} H_{\text{tun},\gamma} H_{\text{tun},\gamma} H_{\text{tun,e}}. \tag{61}$$

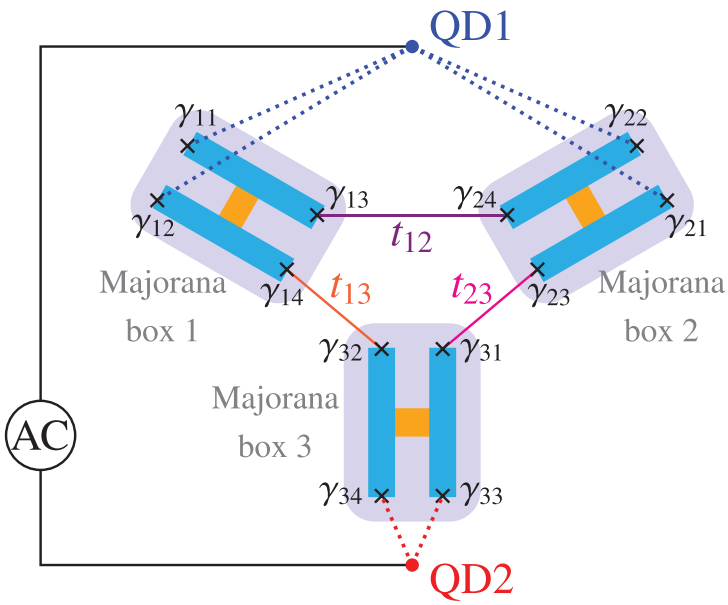

Figure 3. The proposed braiding setup consists of three Majorana boxes mutually linked by tunneling with amplitudes t_{12}, t_{13} and t_{23}. The Majorana operator $\gamma_{n\mu}$ denotes the MBS $\mu \in \{1,\ldots,4\}$ in the box $n \in \{1,2,3\}$. Two QDs (QD1 and QD2) are coupled via tunneling to the MBSs. The quantum dots, the driving field, and the environment remain identical to the case of a single Majorana box. The tunneling couplings are designed for attaining the jump operator (38) whose odd-parity dark states depend on the parameters f and g as shown in equations (39) and (40).

Thus, one can again obtain the effective Hamiltonian as follows,

$$H_{\rm eff} = H_{\rm QD} + H_{\rm env} + H^{\rm RWA}_{\rm drive} + \sum_{r=2}^{4} H^{(r)}_{\rm cot}. \tag{62}$$

This Hamiltonian serves as the starting point for the derivation of the Lindblad equation. Using the Born-Markov approximation, one can trace over the environment degrees of freedom and the quantum dot subspace if the stabilization time is long enough. As shown in appendix C, one finds that the structure of the jump operator is associated with the Kronecker product of Majorana bilinears in each box,

$$\mathcal{S}_{abc} = \mathcal{T}\cdot\left(\chi^1_a \otimes \chi^2_b \otimes \chi^3_c\right)\cdot\mathcal{T}^{-1}, \tag{63}$$

for $a,b,c \in \{0,x,y,z\}$. Here, $\mathcal{T}$ represents a unitary matrix rearranging the blocks in matriceC demonstrates the inclusion of 16 necessary matrices $\mathcal{S}_{abc}$ within the tunneling system depicted in figure 3.

In appendix C, we divide the jump operator of the setup in figure 3 into four contributions $\tilde{K}^{n\nu}_{\rm odd}$ $(n,\nu \in \{1,2\})$, with each superscript corresponding to a specific Majorana bound state as the starting point,

$$\begin{aligned}\tilde{K}^{11}_{\rm odd} = &\left[\lambda_{2,33}e^{i\beta_{2,33}}\left(i\tilde{t}_{12}\tilde{t}_{23}\mathcal{S}^{\rm odd}_{xzx} + i\tilde{t}_{13}\mathcal{S}^{\rm odd}_{y0y}\right)\right.\\ &\left.+\lambda_{2,34}e^{i\beta_{2,34}}\left(i\tilde{t}_{12}\tilde{t}_{23}\mathcal{S}^{\rm odd}_{xzy} - i\tilde{t}_{13}\mathcal{S}^{\rm odd}_{y0x}\right)\right]\lambda_{1,11}e^{-i\beta_{1,11}},\end{aligned} \tag{64}$$

$$\begin{aligned}\tilde{K}^{12}_{\rm odd} = &\left[\lambda_{2,33}e^{i\beta_{2,33}}\left(-i\tilde{t}_{12}\tilde{t}_{23}\mathcal{S}^{\rm odd}_{yzx} + i\tilde{t}_{13}\mathcal{S}^{\rm odd}_{x0y}\right)\right.\\ &\left.-\lambda_{2,34}e^{i\beta_{2,34}}\left(i\tilde{t}_{12}\tilde{t}_{23}\mathcal{S}^{\rm odd}_{yzy} + i\tilde{t}_{13}\mathcal{S}^{\rm odd}_{x0x}\right)\right]\lambda_{1,12}e^{-i\beta_{1,12}},\end{aligned} \tag{65}$$

$$\begin{aligned}\tilde{K}^{21}_{\rm odd} = &\left[\lambda_{2,33}e^{i\beta_{2,33}}\left(-i\tilde{t}_{23}\mathcal{S}^{\rm odd}_{0xx} + i\tilde{t}_{12}\tilde{t}_{13}\mathcal{S}^{\rm odd}_{zyy}\right)\right.\\ &\left.-\lambda_{2,34}e^{i\beta_{2,34}}\left(i\tilde{t}_{23}\mathcal{S}^{\rm odd}_{0xy} + i\tilde{t}_{12}\tilde{t}_{13}\mathcal{S}^{\rm odd}_{zyx}\right)\right]\lambda_{1,21}e^{-i\beta_{1,21}},\end{aligned} \tag{66}$$

$$\begin{aligned}\tilde{K}^{22}_{\rm odd} = &\left[\lambda_{2,33}e^{i\beta_{2,33}}\left(i\tilde{t}_{23}\mathcal{S}^{\rm odd}_{0yx} + i\tilde{t}_{12}\tilde{t}_{13}\mathcal{S}^{\rm odd}_{zxy}\right)\right.\\ &\left.+\lambda_{2,34}e^{i\beta_{2,34}}\left(i\tilde{t}_{23}\mathcal{S}^{\rm odd}_{0yy} - i\tilde{t}_{12}\tilde{t}_{13}\mathcal{S}^{\rm odd}_{zxx}\right)\right]\lambda_{1,22}e^{-i\beta_{1,22}},\end{aligned} \tag{67}$$

where $\mathcal{S}^{\rm odd}_{abc}$ denotes the odd-parity block in $\mathcal{S}_{abc}$. One can thus obtain the jump operator as $\tilde{K}_{\rm odd} = \tilde{K}^{11}_{\rm odd} + \tilde{K}^{12}_{\rm odd} + \tilde{K}^{21}_{\rm odd} + \tilde{K}^{22}_{\rm odd}$.

To approach the structure of the jump operator in equation (38), the tunneling phases are defined as,

$$\begin{aligned}&\beta_{1,11}=\beta_{2,33}+\tfrac{\pi}{2}, \quad \beta_{1,12}=\beta_{2,33}+\pi,\\ &\beta_{1,21}=\beta_{2,33}-\tfrac{\pi}{2}, \quad \beta_{1,22}=\beta_{2,33}+\pi,\ \beta_{2,34}=\beta_{2,33}+\frac{\pi}{2}.\end{aligned} \tag{68}$$

The tunneling amplitudes between the Majorana boxes are set to $t_{12}=(t_{13}+t_{23})/(t_{13}-t_{23})$ for $t_{13}>t_{23}$. Moreover, defining

$$\lambda_{1,1\pm}=\lambda_{1,12}\pm\lambda_{1,11}, \qquad \lambda_{1,2\pm}=\lambda_{1,21}\pm\lambda_{1,22}, \qquad \lambda_{2,3\pm}=\lambda_{2,33}\pm\lambda_{2,34}, \tag{69}$$

the jump operator becomes

$$\tilde{K}_{\text{odd}}=\tfrac{t_{13}^2+t_{23}^2}{t_{23}-t_{13}}\begin{pmatrix}0 & \lambda_{1,2-}\lambda_{2,3-} & -\lambda_{1,1+}\lambda_{2,3-} & 0\\ \lambda_{1,2+}\lambda_{2,3+} & 0 & 0 & \lambda_{1,1+}\lambda_{2,3+}\\ \lambda_{1,1-}\lambda_{2,3+} & 0 & 0 & \lambda_{1,2-}\lambda_{2,3+}\\ 0 & -\lambda_{1,1-}\lambda_{2,3-} & \lambda_{1,2+}\lambda_{2,3-} & 0\end{pmatrix}. \tag{70}$$

For the tunneling amplitude, the last key condition needed to attain the structure of the ideal jump operator (38) is given by,

$$\lambda_{1,1+}\lambda_{1,1-}=\lambda_{1,2+}\lambda_{1,2-}\Leftrightarrow\lambda_{1,12}^2-\lambda_{1,11}^2=\lambda_{1,21}^2-\lambda_{1,22}^2. \tag{71}$$

For simplicity, we introduce the following symbols

$$\tilde{f}\ =\tfrac{\lambda_{1,1+}}{\lambda_{1,2-}}=\tfrac{\lambda_{1,2+}}{\lambda_{1,1-}},\ \tilde{g}=\tfrac{\lambda_{1,2-}}{\lambda_{1,1-}}=\tfrac{\lambda_{1,1+}}{\lambda_{1,2+}}, \tag{72}$$

which allow the jump operator (70) to be written as

$$\tilde{K}_{odd}=\Lambda\begin{pmatrix}0 & \tilde{g}\lambda_{2,3-} & -\tilde{f}\tilde{g}\lambda_{2,3-} & 0\\ \tilde{f}\lambda_{2,3+} & 0 & 0 & \tilde{f}\tilde{g}\lambda_{2,3+}\\ \lambda_{2,3+} & 0 & 0 & \tilde{g}\lambda_{2,3+}\\ 0 & -\lambda_{2,3-} & \tilde{f}\lambda_{2,3-} & 0\end{pmatrix}, \tag{73}$$

with $\Lambda=\lambda_{1,1-}(t_{13}^2+t_{23}^2)/(t_{23}-t_{13})$. If we define $\tilde{f}_1=\tilde{g}\lambda_{2,3-}$, $\tilde{f}_2=-\lambda_{2,3-}$, $\tilde{g}_1=\tilde{f}\lambda_{2,3+}$ and $\tilde{g}_2=\lambda_{2,3+}$, the jump operator $\tilde{K}_{\text{odd}}$ (73) becomes equivalent to the jump operator (38). As anticipated, the dark sates of $\tilde{K}_{\text{odd}}$, $|\tilde{\psi}_1\rangle$ and $|\tilde{\psi}_2\rangle$, take the form given by $|\psi_1\rangle$ (39) and $|\psi_2\rangle$ (40),

$$|\tilde{\psi}_1\rangle\ =\tilde{N}_1\left(-\tilde{g}|001\rangle+|111\rangle\right)\ =\tilde{N}_1\left(\frac{\lambda_{1,22}-\lambda_{1,21}}{\lambda_{1,12}-\lambda_{1,11}}|001\rangle+|111\rangle\right), \tag{74}$$

$$|\tilde{\psi}_2\rangle\ =\tilde{N}_2\left(\tilde{f}|010\rangle+|100\rangle\right)\ =\tilde{N}_2\left(\frac{\lambda_{1,21}+\lambda_{1,22}}{\lambda_{1,12}-\lambda_{1,11}}|010\rangle+|100\rangle\right). \tag{75}$$

From equations (44) and (45), one can find that the other two eigenstates $|\tilde{\psi}_{\pm}\rangle$ of $\tilde{K}_{\text{odd}}$ (73) merge and become a null vector in this case.

Our choice of tunneling amplitudes ensures that the jump operator yields two parameter-dependent dark states within the odd-parity subspace. However, the tunneling system must avoid two scenarios: $\lambda_{2,3+}=0$ and $\lambda_{2,3-}=0$, i.e. the tunneling amplitudes with QD2 cannot be in phase, $\lambda_{2,33}=\lambda_{2,34}$, or exactly out of phase, $\lambda_{2,33}=-\lambda_{2,34}$. Since the dark space only contains one parameter-dependent dark state when $\lambda_{2,3\pm}=0$, this scenario cannot support a braiding transformation. Therefore, we adiabatically vary the tunneling amplitudes $\lambda_{1,2\pm}$ while keeping $\lambda_{2,3\pm}$ as a non-vanishing constant during braiding.

4.4. The braiding transformation

The parameters $\lambda_{1,2\pm}$ are changed adiabatically, and $\lambda_{1,1\pm}$ changes accordingly due to equation (71). With the time-periodic boundary condition from time t_0 to t_f, we establish the following polar coordinate systems for the tunnel amplitudes,

$$\lambda_{1,2-}(t)=r_2\sin[\theta_2(t)], \qquad \lambda_{1,2+}(t)=r_2\cos[\theta_2(t)]; \tag{76}$$

$$\lambda_{1,1-}(t)=r_1\cos[\theta_1(t)], \qquad \lambda_{1,1+}(t)=r_1\sin[\theta_1(t)], \tag{77}$$

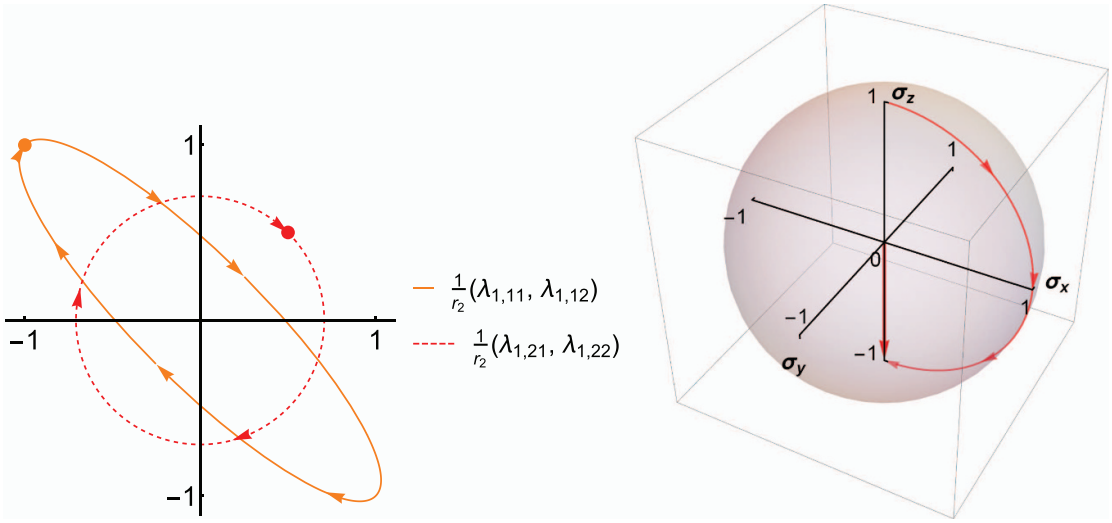

Figure 4. The left diagram shows how the tunneling amplitudes vary from $\theta_2(t_0) = 0$ to $\theta_2(t_f) = 2\pi$ when $r_1 = 2r_2$ and $\theta_1(t) = \theta_2(t)$ in equations (76) and (77). The solid dots in the cyclic adiabatic evolution represent the initial and final values of the parameters. The Bloch vector $\tilde{\boldsymbol{n}} = (\sin[\theta_2/2], 0, \cos[\theta_2/2])$ undergoes the rotation depicted in the right figure.

where $\theta_l(t_f) = \theta_l(t_0) + 2\pi$ for $l \in \{1, 2\}$. The equation $r_2^2 \cos(\theta_2)\sin(\theta_2) \equiv r_1^2 \cos(\theta_1)\sin(\theta_1)$ must be satisfied because of the given requirement as shown in equation (71).

As shown in section 4.2, the pure steady state $\tilde{\rho}_s$ in this setup can be formulated as ρ_s in equation (48). Analogously to the function $F(f, g)$ (52) in the steady state ρ_s, the function $\tilde{F}$ in this case is then translated into

$$\tilde{F}(\lambda_{1,21}, \lambda_{1,22}) = \sin\left[\frac{1}{4}\sin^{-1}\left(\frac{\lambda_{1,21} - \lambda_{1,22}}{\sqrt{2\lambda_{1,21}^2 + 2\lambda_{1,22}^2}}\right)\right]. \tag{78}$$

Using equation (76) and (77), one can express $\tilde{F}$ as a function of θ_2 as $\tilde{F}(\theta_2) = \sin(\theta_2/4)$. Referring to the definition of the Bloch vector in equation (49), this results in $\tilde{\boldsymbol{n}} = (\sin[\theta_2/2], 0, \cos[\theta_2/2])$. As anticipated, the Bloch vector is parametrized by θ_2, indicating its dependence on θ_2 rather than time t. The steady state with this Bloch vector reaches $|\tilde{\psi}_2\rangle$ from $|\tilde{\psi}_1\rangle$ after the parameters have been varied along one cycle. This process thus gives rise to the braiding operator $B = \sigma_y$ as described in equation (54).

In figure 4, we present a numerical example where $r_1 = 2r_2$ and $\theta_1(t) = \theta_2(t)$, with θ linearly varying with time. This figure shows the trajectory of the Bloch vector alongside the periodic change in parameters.

To summarize, in this section, we first ascertained that braiding requires a minimum of three Majorana boxes, which collectively form an open quantum system potentially possessing two parameter-dependent dark states with the same parity. In section 4.1, we introduced the ideal jump operator (38), which encompasses two dark states (39) and (40) within the odd-parity subspace. Following the Lindblad equation with this jump operator, the dissipation should lead the reduced system into a state within the subspace spanned exclusively by these two dark states, as depicted in equations (46) and (48). To preserve the chiral symmetry in the steady state, the function F in equation (48) must be real and must obey $F \in [-1,\ 1]$. Due to the presence of chiral symmetry, topological order emerges in the steady state, characterized by the Bloch vector (49) described in section 4.2.

Based on the ideal jump operator (38), we constructed the tunneling system depicted in figure 3, which represents the simplest setup leading to the desired structure of the ideal jump operator. By an appropriate choice of tunneling parameters, the jump operator (73) in the setup of figure 3 has two parameter-dependent and odd-parity dark states as shown in equations (74)–(75). However, one should keep in mind to avoid in-phase and opposite-phase tunneling amplitudes between QD 2 and MBSs, i.e. $\lambda_{2,33} \neq \pm\lambda_{2,34}$ because in either of these cases braiding is not feasible.

In this section, we have focused on the simplest device which allows braiding of two driven-dissipative Majorana box qubits. However, we would like to point out that the proposed architecture can be straightforwardly extended to a larger number of qubits by increasing the number of coupled Majorana box qubits. This would make it possible to form a network of topological qubits and implement braiding between all adjacent qubits, thus enabling more general computing gates.

Experimentally detecting the successful braiding requires reading out the qubit state. For this purpose, a quantum-dot-based readout method can be used [76]. This approach employs multiple QDs and a gate switch to align their energy levels by bringing them into resonance. Our proposed setup, which is designed for qubit braiding, is advantageous in this respect because it can be seamlessly adapted for qubit readout. Since the readout protocol aligns with the approximations we used for braiding, both the braiding and readout processes can be conducted within the same configuration and under identical conditions.

5. Conclusion

We have considered a driven-dissipative system consisting of Majorana box quits. In such a system, the MBSs are coupled via electron tunneling to QDs, which are in turn driven by an applied AC voltage. Dissipation is brought about by the coupling to the electromagnetic environment. It had been shown before that this combination of drive and dissipation can stabilize certain Majorana qubit states as dark states of the corresponding Lindblad equation.

We have considered the question of whether topological transformations, i.e. braiding, can be executed within such a dark-state subspace. In a non-Abelian exchange due to braiding, rotations between different, degenerate qubit states are achieved due to an adiabatic change of system parameters. In this context, these parameters represent the tunneling amplitudes between QDs and MBSs. Moreover, the result of the braiding transformation should be topological, in the sense that it depends only on the topological winding number of the parameter path.

We showed that such a braiding transformation is indeed possible in a driven-dissipative Majorana box system consisting of three Majorana boxes. The latter contains a four-dimensional odd-parity subspace. Moreover, for a suitable choice of tunneling couplings, such a system can host a two-dimensional dark-state subspace in which a braiding transformation can be implemented. To achieve such braiding, certain parameters of the system have to be tuned to special symmetric values. However, the remaining free parameters still allow an adiabatic change of parameters along closed loops in parameter space, and the resulting braiding transformation is topological in this reduced parameter space.

Data availability statement

All data that support the findings of this study are included within the article (and any supplementary files).

Acknowledgments

The authors would like to acknowledge useful discussions with Johan Ekström. SSK acknowledges financial support from the National Research Fund Luxembourg under Grant C18/MS/12704391/QUTHERM.

Appendix A. The solid angle

When the parameters are driven by time-periodic functions from $t = t_0$ to $t = t_f$, one obtains the solid angle given in equation (26). The Bloch vector (24) has unit length and is orthogonal to the vector $\boldsymbol{a} = (0, 1, 0)$. The solid angle can then be calculated as follows,

$$\Omega = \int_{t_0}^{t_f} \mathrm{d}t\ [\boldsymbol{n}(k_x, k_z) \times \partial_t \boldsymbol{n}(k_x, k_z)] \cdot \boldsymbol{a} = \int_{t_0}^{t_f} \mathrm{d}t\,(n_z \partial_t n_x - n_x \partial_t n_z)\,. \tag{A.1}$$

Due to $n_x^2 + n_z^2 = 1$, we can introduce polar coordinates, $n_x(t) = \sin\Theta(t)$ and $n_z(t) = \cos\Theta(t)$. Then, we find

$$\begin{aligned}\partial_t \ln\left(e^{i\Theta}\right) &= \partial_t \ln(n_z + i n_x) = \frac{1}{n_z + i n_x}\partial_t (n_z + i n_x) \\ &= \frac{n_z - i n_x}{n_z^2 + n_x^2}\partial_t (n_z + i n_x) = i\,(n_z \partial_t n_x - n_x \partial_t n_z)\,.\end{aligned} \tag{A.2}$$

Using this in the integral of the solid angle, we have

$$\Omega = -i \int_{t_0}^{t_f} \mathrm{d}t\ \partial_t \ln\left(e^{i\Theta}\right) = \int_{t_0}^{t_f} \mathrm{d}t\ \partial_t \Theta(t) = \Theta\left(t_f\right) - \Theta(t_0)\,, \tag{A.3}$$

where $\Theta(t) = \arctan(n_x/n_z) = -\arctan(k_z/k_x)$.

Appendix B. Stabilization of three entangled Majorana boxes in the odd-parity subspace

As shown in section 4.1, we only need to focus on the dissipation in the odd-parity sector, which corresponds to the manifold of the four odd-parity states $|001\rangle$, $|010\rangle$, $|100\rangle$ and $|111\rangle$. Without loss of generality, we can express an arbitrary 4×4 density matrix as follows,

$$\rho \quad = \sum_{n=0}^{3} a_{nn}\,|n\rangle\langle n| + \sum_{n>m}\left[(a_{nm}+i\,b_{nm})\,|n\rangle\langle m| + \text{h.c.}\right], \tag{B.1}$$

where a_{nm} and b_{nm} are real numbers and where $\{|0\rangle, |1\rangle, |2\rangle, |3\rangle\}$ are shorthands for the four odd-parity states. The matrix coefficients should satisfy $\sum_n a_{nn}\equiv 1$ and $a_{nn}\geqslant 0$ for $n\in\{0,1,2,3\}$.

Using the jump operator (38), the Lindblad operator $\mathcal{L}[K_{\text{odd}}]$ drives the reduced system to the steady state ρ_s when $\mathcal{L}[K_{\text{odd}}]\rho_s = 0$. This condition dictates that the elements of the steady state density matrix should obey, in the case of the diagonal elements,

$$\begin{aligned} a_{00} &= -g a_{03}, \quad & a_{11} &= \frac{f^2\left(a_{03}g^2 + a_{03} + g\right)}{(f^2+1)\,g}, \\ a_{33} &= -\tfrac{a_{03}}{g}, \quad & a_{22} &= \frac{a_{03}g^2 + a_{03} + g}{f^2 g + g}, \end{aligned} \tag{B.2}$$

and for the off-diagonal elements,

$$a_{01} = -fg a_{23},\ a_{02} = -g a_{23},\ a_{13} = f a_{23},\ \tfrac{1+f^2}{f}a_{12} + \tfrac{1+g^2}{-g}a_{03} = 1; \tag{B.3}$$

$$b_{01} = fg b_{23},\ b_{02} = g b_{23},\ b_{03} = b_{12} = 0,\ b_{13} = f b_{23}. \tag{B.4}$$

We can define a function $F(f,g)\in[-1,1]$ to replace a_{12} and a_{03} in the steady state as the following expressions,

$$a_{12} = f^2\frac{f}{1+f^2} \text{ and } a_{03} = \left(1-f^2\right)\frac{-g}{1+g^2}, \tag{B.5}$$

such that it satisfies the last equation in equation (B.3). Then, one finds the following general form of the steady state density matrix in the odd-parity subspace,

$$\rho_s = \begin{pmatrix} \frac{(1-f^2)g^2}{g^2+1} & fg(-a_{23}+ib_{23}) & g(-a_{23}+ib_{23}) & \frac{(f^2-1)g}{g^2+1} \\ fg(-a_{23}-ib_{23}) & \frac{f^2f^2}{f^2+1} & \frac{ff^2}{f^2+1} & f(a_{23}+ib_{23}) \\ g(-a_{23}-ib_{23}) & \frac{ff^2}{f^2+1} & \frac{f^2}{f^2+1} & a_{23}+ib_{23} \\ \frac{(f^2-1)g}{g^2+1} & f(a_{23}-ib_{23}) & a_{23}-ib_{23} & \frac{1-f^2}{g^2+1} \end{pmatrix}. \tag{B.6}$$

This dissipation should stabilize the two dark states in equations (39) and (40). We thus change the basis of the steady state (B.6) using,

$$\begin{aligned} U &= \left(|\psi_1\rangle\ |\psi_2\rangle\ |\psi_3\rangle\ |\psi_4\rangle\right) \\ &= \begin{pmatrix} -g/\sqrt{1+g^2} & 0 & 1/\sqrt{1+g^2} & 0 \\ 0 & f/\sqrt{1+f^2} & 0 & -1/\sqrt{1+f^2} \\ 0 & 1/\sqrt{1+f^2} & 0 & f/\sqrt{1+f^2} \\ 1/\sqrt{1+g^2} & 0 & g/\sqrt{1+g^2} & 0 \end{pmatrix}, \end{aligned} \tag{B.7}$$

where $|\psi_1\rangle$ and $|\psi_2\rangle$ are the dark states (39) and (40), and $|\psi_3\rangle$ (44) and $|\psi_4\rangle$ (45) satisfy $\rho_s|\psi_3\rangle = \rho_s|\psi_4\rangle = 0$. The vectors $|\psi_3\rangle$ and $|\psi_4\rangle$ are found by diagonalizing ρ_s (B.6). As anticipated, ρ_s is a semidefinite matrix with two zero eigenvalues, because the dark space consists of only two dark states. In this basis, all components of the steady state density matrix should vanish except those in the subspace of $\{|\psi_1\rangle,\ |\psi_2\rangle\}$. Therefore,

$$\begin{aligned} \rho_s = \left(1-f^2\right)|\psi_1\rangle\langle\psi_1| + r_{23}e^{-i\theta_{23}}\sqrt{(f^2+1)\,(g^2+1)}|\psi_1\rangle\langle\psi_2| \\ + r_{23}e^{i\theta_{23}}\sqrt{(f^2+1)\,(g^2+1)}|\psi_2\rangle\langle\psi_1| + f^2|\psi_2\rangle\langle\psi_2|, \end{aligned} \tag{B.8}$$

where $r_{23} = \mathrm{sgn}(a_{23})\sqrt{a_{23}+b_{23}}$ and $\theta_{23} = \arctan(b_{23}/a_{23})$ with $\theta_{23} \in [0,\ \pi)$. To get a pure state, we can define r_{23} as follows,

$$r_{23} = \frac{F\sqrt{1-f^2}}{\sqrt{(f^2+1)(g^2+1)}}. \tag{B.9}$$

As expected, the pure state becomes the combination of the two dark states $|\psi_1\rangle$ and $|\psi_2\rangle$,

$$\rho_s = \left(\sqrt{1-F^2}e^{i\alpha_1}|\psi_1\rangle + Fe^{i\alpha_2}|\psi_2\rangle\right) \otimes \text{h.c.} \tag{B.10}$$

where $\alpha_1 - \alpha_2 = \theta_{23}$, and we assumed that F and r_{23} have the same sign.

To ensure a pure state with chiral symmetry, one possibility is to choose $\theta_{23} = 0$, or $b_{23} = 0$ and $a_{23}^2 = (f^2 - F^4)/[(f^2+1)(g^2+1)]$. This can be done by changing the relative phase between the two dark states $|\psi_1\rangle$ and $|\psi_2\rangle$. Then, the steady state (B.8) becomes

$$\begin{aligned}\rho_s = &\left(1-f^2\right)|\psi_1\rangle\langle\psi_1| + F\sqrt{1-f^2}\,|\psi_1\rangle\langle\psi_2| \\ &+ F\sqrt{1-f^2}\,|\psi_2\rangle\langle\psi_1| + f^2|\psi_2\rangle\langle\psi_2|,\end{aligned} \tag{B.11}$$

whose Bloch vector $(2F\sqrt{1-f^2}, 0, 1-2f^2)$ rotates in the $x-z$ plane.

Appendix C. The jump operator in the tunneling system of three entangled Majorana boxes

To determine the corresponding jump operators in a system with three Majorana boxes, we generalize the derivation presented in section 2.1, i.e. we apply a SW transformation to the tunneling Hamiltonian to obtain an effective cotunneling Hamiltonian. Subsequently, we can extract the operator in the Majorana sector which becomes the jump operator after tracing over the other degrees of freedom within a Born-Markov approximation.

In the case of three Majorana boxes, the Hamiltonian of the open system is given by

$$H(t) = H_{\text{box}} + H_{\text{QD}} + H_{\text{env}} + H_{\text{drive}}(t) + H_{\text{tun,e}} + H_{\text{tun},\gamma}, \tag{C.1}$$

where H_{box}, H_{QD}, H_{env}, and $H_{\text{drive}}(t)$ represent the Hamiltonian of the Majorana box, QDs, environment, and the time-dependent driving field, respectively. For three Majorana boxes, $H_{\text{box}} = E_C\sum_{n=1}^{3}(\hat{N}_n - N_g)^2$. The tunneling Hamiltonian consists of two contributions. Electron tunneling between the QDs and Majorana box n is represented by,

$$H_{\text{tun,e}} \quad = t_0\sum_{n=1}^{3}\sum_{j=1}^{2}\sum_{\mu=1}^{4}\lambda_{j,n\mu}e^{-i\beta_{j,n\mu}}e^{-i\hat{\phi}_n + i\delta_j + i\epsilon_j t}d_j^\dagger\gamma_{n\mu} + \text{h.c.}, \tag{C.2}$$

where direct tunneling between the two Majorana boxes (the box n and the box n') is described by,

$$H_{\text{tun},\gamma} \quad = E_C\sum_{n,n'=1}^{3}\sum_{\mu,\nu=1}^{4} i\tilde{t}_{nn'}\gamma_{n\mu}\gamma_{n'\nu}, \tag{C.3}$$

where the dimensionless parameter $\tilde{t}_{nn'} = t_{nn'}/E_C$ and $t_{nn'}$ is the tunnel coupling energy between the boxes n and n'. Here, we assume that $t_{nn} = 0$ and $t_{nn'} > 0$ for all amplitudes.

To perform the SW transformation, we once again assume the energy scales of tunnel couplings, t_0 and $t_{nn'}$, to be small. Applying the RWA to remove fast oscillating terms in the driving Hamiltonian, the unperturbed Hamiltonian becomes time-independent and can be expressed as follows,

$$\begin{aligned}H_0 &= H_{\text{box}} + H_{\text{QD}} + H_{\text{env}} + H_{\text{drive}} \\ &= E_C\sum_n\left(\hat{N}_n - N_g\right)^2 + \sum_{j=1,2}\epsilon_j d_j^\dagger d_j + \sum_m E_m b_m^\dagger b_m + \mathcal{A}\left(d_2^\dagger d_1 + h.c.\right),\end{aligned} \tag{C.4}$$

where $\mathcal{A}$ is the amplitude of the driving field.

We perform an SW transformation to the effective Hamiltonian $H_{\text{eff}} = e^S(H_0 + H_{\text{tun}})e^{-S}$ where $H_{\text{tun}} = H_{\text{tun,e}} + H_{\text{tun},\gamma}$. For three Majorana boxes, it is necessary to go up to the fourth order in the expansion,

$$\begin{aligned}H_{\text{eff}} \quad \approx\ & H_0 + H_{\text{tun}} + [S, H_0] + [S, H_{\text{tun}}] + \tfrac{1}{2}[S,[S,H_0]] + \tfrac{1}{2}[S,[S,H_{\text{tun}}]] \\ &+ \tfrac{1}{6}[S,[S,[S,H_0]]] + \tfrac{1}{6}[S,[S,[S,H_{\text{tun}}]]] + \tfrac{1}{24}[S,[S,[S,[S,H_0]]]].\end{aligned} \tag{C.5}$$

In the SW transformation, the Hamiltonian can be diagonalized to first order in the perturbation by finding a generator S which satisfies,

$$H_{\text{tun}} = -[S, H_0]\,. \tag{C.6}$$

With this generator the expansion becomes,

$$H_{\text{eff}} \approx H_0 + \tfrac{1}{2}[S, H_{\text{tun}}] + \tfrac{1}{3}[S,[S, H_{\text{tun}}]] + \tfrac{1}{8}[S,[S,[S, H_{\text{tun}}]]]\,. \tag{C.7}$$

To find the generator S satisfying equation (C.6) explicitly, it is convenient to diagonalize the Hamiltonian H_0 (C.4). If we write H_0 in a block-diagonal form, we only need to diagonalize it in the subspace of the quantum dot operators because H_{box} and H_{env} are already diagonal matrices. One finds ,

$$H_{\text{QD}} + H_{\text{drive}} = \begin{pmatrix} \epsilon_1 & 0 & 0 & \mathcal{A} \\ 0 & -\epsilon_1 & -\mathcal{A} & 0 \\ 0 & -\mathcal{A} & -\epsilon_2 & 0 \\ \mathcal{A} & 0 & 0 & \epsilon_2 \end{pmatrix} = U_0 H_d U_0^{-1}, \tag{C.8}$$

where $H_d = \text{diag}(-\eta_+, \eta_-, -\eta_-, \eta_+)$ and

$$U_0 = \begin{pmatrix} 0 & \frac{\eta_+ - 2\epsilon_2}{\sqrt{(\eta_+ - 2\epsilon_2)^2 + 4\mathcal{A}^2}} & \frac{2\mathcal{A}}{\sqrt{(\eta_+ - 2\epsilon_2)^2 + 4\mathcal{A}^2}} & 0 \\ \frac{\eta_- - 2\epsilon_2}{\sqrt{(\eta_+ - 2\epsilon_1)^2 + 4\mathcal{A}^2}} & 0 & 0 & \frac{2\mathcal{A}}{\sqrt{(\eta_+ - 2\epsilon_1)^2 + 4\mathcal{A}^2}} \\ 0 & \frac{\eta_- - 2\epsilon_2}{\sqrt{(\eta_+ - 2\epsilon_1)^2 + 4\mathcal{A}^2}} & \frac{2\mathcal{A}}{\sqrt{(\eta_+ - 2\epsilon_1)^2 + 4\mathcal{A}^2}} & 0 \\ \frac{\eta_+ - 2\epsilon_2}{\sqrt{(\eta_+ - 2\epsilon_2)^2 + 4\mathcal{A}^2}} & 0 & 0 & \frac{2\mathcal{A}}{\sqrt{(\eta_+ - 2\epsilon_2)^2 + 4\mathcal{A}^2}} \end{pmatrix}. \tag{C.9}$$

The elements of the diagonal matrix are given by $\eta_\pm = (\epsilon_1 + \epsilon_2 \pm \sqrt{4\mathcal{A}^2 + (\epsilon_1 - \epsilon_2)^2})/2$. Subsequently, the total Hamiltonian is transformed into this new basis, and the effective Hamiltonian is found to be

$$H'_{\text{eff}} = e^S (H'_0 + H'_{\text{tun}})\, e^{-S}, \tag{C.10}$$

where $H'_0 = U_0 H_0 U_0^{-1}$ and $H'_{\text{tun}} = U_0 H_{\text{tun}} U_0^{-1}$. For the diagonal matrix H'_0, the components of the commutator in equation (C.6) can be written as

$$(H'_{\text{tun}})_{jk} = -[S, H'_0]_{jk} = \left(\epsilon'_j - \epsilon'_k\right) S_{jk}, \tag{C.11}$$

where ϵ'_j and ϵ'_k are the diagonal elements in H'_0, which depend on E_C, E_m, and $\eta_\pm$ in the subspace of MBSs, bath, and QDs, respectively. Using this to determine S, one can perform the SW transformation in equation (C.7). For the second-order term, one finds, as they are in a different basis,

$$\begin{aligned} \left(H'^{(2)}_{\text{cot}}\right)_{jk} &= \frac{1}{2}[S, H'_{\text{tun}}]_{jk} \\ &= \frac{1}{2}\sum_l (H'_{\text{tun}})_{jl}(H'_{\text{tun}})_{lk}\left(\frac{1}{\epsilon'_k - \epsilon'_k} + \frac{1}{\epsilon'_k - \epsilon'_k}\right). \end{aligned} \tag{C.12}$$

The low-energy regime imposes the condition that no energy scale exceeds the charging energy E_C and the superconductivity gap Δ. Therefore, the second-order term can be approximated as,

$$\left(H'^{(2)}_{\text{cot}}\right)_{jk} \approx \frac{1}{E_C}\left(U_0 H_{\text{tun}} H_{\text{tun}} U_0^{-1}\right)_{jk}. \tag{C.13}$$

For the third-order term in the expansion (C.7), one can use the second-order term and finds,

$$\begin{aligned} \left(H'^{(3)}_{\text{cot}}\right)_{jk} &= \frac{1}{3}[S,[S, H'_{\text{tun}}]]_{jk} = \frac{1}{3}\left[S, 2H^{(2)}_{\text{cot}}\right]_{jk} \\ &= \frac{2}{3E_C}\sum_l (H'_{\text{tun}})_{jl}(H'_{\text{tun}} H'_{\text{tun}})_{lk}\left[\frac{1}{\epsilon'_j - \epsilon'_l} + \frac{1}{\epsilon'_k - \epsilon'_l}\right]. \end{aligned} \tag{C.14}$$

In the low-energy regime, one can again approximate the third term as,

$$\left(H'^{(3)}_{\text{cot}}\right)_{jk} \approx \frac{4}{3E_C^2}\left(U_0 H_{\text{tun}} H_{\text{tun}} H_{\text{tun}} U_0^{-1}\right)_{jk}. \tag{C.15}$$

Using the same method leads to the fourth term as follows,

$$\left(H_{\rm cot}^{\prime(4)}\right)_{jk} \approx \frac{1}{E_C^3}\left[U_0\left(H_{\rm tun}\right)^4 U_0^{-1}\right]_{jk}. \tag{C.16}$$

In the case of three Majorana boxes, the cotunneling Hamiltonian is obtained in the basis before the diagonalization of H_0,

$$H_{\rm cot} = \sum_{r=2}^{4}\left(\frac{1}{(r-1)!}-\frac{1}{r!}\right)\left(\frac{2}{E_C}\right)^{r-1}\left(H_{\rm tun}\right)^r. \tag{C.17}$$

However, some terms in the above formula do not describe full trajectories between the two QDs. For instance, because $H_{\rm tun} = H_{\rm tun,e} + H_{\rm tun,\gamma}$, $H_{\rm cot}^{(2)}$ turns into,

$$\begin{aligned}\frac{1}{E_C}\left(H_{\rm tun}H_{\rm tun}\right) = \frac{1}{E_C}\big(&H_{\rm tun,e}H_{\rm tun,e} + H_{\rm tun,e}H_{\rm tun,\gamma}\\ &+H_{\rm tun,\gamma}H_{\rm tun,e} + H_{\rm tun,\gamma}H_{\rm tun,\gamma}\big).\end{aligned} \tag{C.18}$$

Only the first term, $(H_{\rm tun,e}H_{\rm tun,e})$, describes a complete trajectory between the two dots, similar to the scenario of a single Majorana box. Terms containing incomplete trajectories would only lead to subleading corrections to higher-order tunneling processes. Therefore, retaining only this term to second order, we find the second-order cotunneling Hamiltonian,

$$H_{\rm cot}^{(2)} \approx \frac{t_0^2}{E_C}\sum_n \left(e^{i\delta_{12}+i\epsilon_{21}t}A_{12}^n d_2^\dagger d_1 + {\rm h.c.}\right). \tag{C.19}$$

The operator A_{jk}^n denotes the dynamics within the Majorana box n, where the transport occurs between QDs j and k,

$$A_{jk}^n = \textstyle\sum_{\mu<\nu}\Lambda_{jk}^{n\mu,n\nu}\gamma_{n\mu}\gamma_{n\nu}, \tag{C.20}$$

$$\Lambda_{jk}^{n\mu,n\nu} = \lambda_{j,n\mu}\lambda_{k,n\nu}e^{i\left(\beta_{k,n\nu}-\beta_{j,n\mu}\right)} - \lambda_{j,n\nu}\lambda_{k,n\mu}e^{i\left(\beta_{k,n\mu}-\beta_{j,n\nu}\right)}. \tag{C.21}$$

The subscript $n \in \{1,\ ,2,\ 3\}$ indicates the box, and $j,\ k \in \{1,\ 2\}$ represent the QDs. The complex parameter $\Lambda_{jk}^{n\mu,n\nu}$ contains the tunnel couplings between QDs j, k and MBSs $\gamma_{n\mu}$ and $\gamma_{n\nu}$.

For the third-order term, one can find the complete transport between two dots as

$$H_{\rm cot}^{(3)} \approx \tfrac{4}{3E_C^2}H_{\rm tun,e}H_{\rm tun,\gamma}H_{\rm tun,e} = \tfrac{4t_0^2}{3E_C}\textstyle\sum_{n\neq n'}\left(e^{i\delta_{12}+i\epsilon_{21}t}A_{12}^{n,n'}d_2^\dagger d_1 + {\rm h.c.}\right), \tag{C.22}$$

$$\text{where } A_{jk}^{n,n'} = i\tilde{t}_{n,n'}\textstyle\sum_{\mu<\nu}\sum_{\mu'<\nu'}\Lambda_{jk}^{n\mu,n'\nu'}\gamma_{n\mu}\gamma_{n\nu}\gamma_{n'\mu'}\gamma_{n'\nu'}. \tag{C.23}$$

In the operator $A_{jk}^{n,n'}$ (C.23), the trajectory starts from quantum dot j, goes to Majorana box n, then proceeds to Majorana box n' through the tunnel between the MBSs $\gamma_{n\nu}$ and $\gamma_{n'\mu'}$, and finally reaches quantum dot k. For the fourth order, the complete transport is written as,

$$\begin{aligned}H_{\rm cot}^{(4)} &\approx \frac{1}{E_C^3}H_{\rm tun,e}H_{\rm tun,\gamma}H_{\rm tun,\gamma}H_{\rm tun,e}\\ &= \frac{t_0^2}{E_C}\sum_{n\neq n'\neq n''}\left(e^{i\delta_{12}+i_{21}t}A_{12}^{n,n',n''}d_2^\dagger d_1 + {\rm h.c.}\right)\end{aligned} \tag{C.24}$$

$$\text{where } A_{jk}^{n,n',n''} = -\tilde{t}_{n,n'}\tilde{t}_{n',n''}\sum_{\mu<\nu}\sum_{\mu'<\nu'}\sum_{\mu''<\nu''}\Lambda_{jk}^{n\mu,n''\nu''}\gamma_{n\mu}\gamma_{n\nu}\gamma_{n'\mu'}\gamma_{n'\nu'}\gamma_{n''\mu''}\gamma_{n''\nu''}. \tag{C.25}$$

The trajectory in the fourth-order term involves three boxes n, n', and n''. Combining these three perturbation terms in equations (C.19), (C.22) and (C.24), one can obtain the cotunneling Hamiltonian from the SW transformation. Furthermore, it is observed that the operators A_{jk} in equations (C.20), (C.23), and (C.25) serve as the building blocks for the jump operator in the Lindblad equation of the Majorana section after applying the Born-Markov approximation.

In an open system like figure 3, the following Majorana bilinears represent the corresponding Pauli operators of resulting in the Majorana box n,

$$\chi_x^n = i\gamma_{n2}\gamma_{n4}, \qquad \chi_y^n = i\gamma_{n3}\gamma_{n2}, \qquad \chi_z^n = i\gamma_{n4}\gamma_{n3}. \tag{C.26}$$

For simplicity in the subsequent calculation, we define a matrix $\mathcal{S}_{abc}$ as follows,

$$\mathcal{S}_{abc} = \mathcal{T}\cdot\left(\chi_a^1\otimes\chi_b^2\otimes\chi_c^3\right)\cdot\mathcal{T}^{-1},\ \text{for}\ a,\ b,\ c\in\{0,\ x,\ y,\ z\}, \tag{C.27}$$

where $\mathcal{T}$ is the unitary matrix rearranging the blocks in matrices according to the parity.

For three entangled boxes, there exist 4^3 distinct $\mathcal{S}_{abc}$ matrices. However, certain matrices within this set vanish in the single-parity subspace, necessitating the exclusion of these trajectories since braiding does not change the parity of states. Through algebraic manipulations, one can identify a total of 16 associated trajectories, with their corresponding $\mathcal{S}_{abc}$ matrices encompassed in the set S as outlined below,

$$\begin{aligned}\mathcal{S}_{abc} &= \mathcal{T}\left(\chi_a^1\otimes\chi_b^2\otimes\chi_c^3\right)\mathcal{T}^{\dagger}, \text{where}\ (a,b,c)\in s,\\ \text{and}\ s = \{&(0,x,x),\ (0,x,y),\ (0,y,x),\ (0,y,y),\\ &(x,0,x),\ (x,0,y),\ (x,z,x),\ (x,z,y),\\ &(y,0,x),\ (y,0,y),\ (y,z,x),\ (y,z,y),\\ &(z,x,x),\ (z,x,y),\ (z,y,x),\ (z,y,y)\}.\end{aligned} \tag{C.28}$$

Utilizing these 16 trajectories, the tunneling system has been constructed as figure 3 in section 4.3.

To calculate the jump operator in the tunneling system illustrated in figure 3, our focus is on the odd-parity subspace of MBSs exclusively. Considering the four tunnels originating from QD 1 and connecting to Majorana qubits, we partition the odd-parity tunneling matrix $\tilde{K}_{\text{odd}}$ into four contributions: $\tilde{K}_{\text{odd}}^{11}$, $\tilde{K}_{\text{odd}}^{12}$, $\tilde{K}_{\text{odd}}^{21}$ and $\tilde{K}_{\text{odd}}^{22}$, with each superscript corresponding to a specific Majorana bound state. For instance, the computation of $\tilde{K}_{\text{odd}}^{11}$ can be visualized using the following tree diagram,

$$\gamma_{11}\begin{cases}\nearrow\gamma_{13}\xrightarrow{t_{12}}\gamma_{24}\gamma_{23}\xrightarrow{t_{23}}\gamma_{31}\begin{cases}\nearrow\gamma_{33}\\ \searrow\gamma_{34}\end{cases}\\ \searrow\gamma_{14}\xrightarrow{t_{13}}\gamma_{32}\begin{cases}\nearrow\gamma_{33}\\ \searrow\gamma_{34}\end{cases}\end{cases}. \tag{C.29}$$

From the operators $A_{jk}^{n,n'}$ (C.23) and $A_{jk}^{n,n',n''}$ (C.25), one can express $\tilde{K}_{\text{odd}}^{11}$ as

$$\tilde{K}_{\text{odd}}^{11} = A_{12}^{1,3} + A_{12}^{1,2,3} \tag{C.30}$$

$$\begin{aligned}\tilde{K}_{\text{odd}}^{11} = \Big[&\lambda_{2,33}e^{i\beta_{2,33}}\left(i\tilde{t}_{12}\tilde{t}_{23}\mathcal{S}_{xzx}^{\text{odd}} + i\tilde{t}_{13}\mathcal{S}_{y0y}^{\text{odd}}\right)\\ &+\lambda_{2,34}e^{i\beta_{2,34}}\left(i\tilde{t}_{12}\tilde{t}_{23}\mathcal{S}_{xzy}^{\text{odd}} - i\tilde{t}_{13}\mathcal{S}_{y0x}^{\text{odd}}\right)\Big]\lambda_{1,11}e^{-i\beta_{1,11}},\end{aligned} \tag{C.31}$$

where $\mathcal{S}_{abc}^{\text{odd}}$ denotes the odd-parity block in $\mathcal{S}_{abc}$. Applying the same method, the rest of the contributions in the jump operator $\tilde{K}_{\text{odd}}$ are formulated as follows,

$$\begin{aligned}\tilde{K}_{\text{odd}}^{12} = \Big[&\lambda_{2,33}e^{i\beta_{2,33}}\left(-i\tilde{t}_{12}\tilde{t}_{23}\mathcal{S}_{yzx}^{\text{odd}} + i\tilde{t}_{13}\mathcal{S}_{x0y}^{\text{odd}}\right)\\ &-\lambda_{2,34}e^{i\beta_{2,34}}\left(i\tilde{t}_{12}\tilde{t}_{23}\mathcal{S}_{yzy}^{\text{odd}} + i\tilde{t}_{13}\mathcal{S}_{x0x}^{\text{odd}}\right)\Big]\lambda_{1,12}e^{-i\beta_{1,12}},\end{aligned} \tag{C.32}$$

$$\begin{aligned}\tilde{K}_{\text{odd}}^{21} = \Big[&\lambda_{2,33}e^{i\beta_{2,33}}\left(-i\tilde{t}_{23}\mathcal{S}_{0xx}^{\text{odd}} + i\tilde{t}_{12}\tilde{t}_{13}\mathcal{S}_{zyy}^{\text{odd}}\right)\\ &-\lambda_{2,34}e^{i\beta_{2,34}}\left(i\tilde{t}_{23}\mathcal{S}_{0xy}^{\text{odd}} + i\tilde{t}_{12}\tilde{t}_{13}\mathcal{S}_{zyx}^{\text{odd}}\right)\Big]\lambda_{1,21}e^{-i\beta_{1,21}},\end{aligned} \tag{C.33}$$

$$\begin{aligned}\tilde{K}_{\text{odd}}^{22} = \Big[&\lambda_{2,33}e^{i\beta_{2,33}}\left(i\tilde{t}_{23}\mathcal{S}_{0yx}^{\text{odd}} + i\tilde{t}_{12}\tilde{t}_{13}\mathcal{S}_{zxy}^{\text{odd}}\right)\\ &+\lambda_{2,34}e^{i\beta_{2,34}}\left(i\tilde{t}_{23}\mathcal{S}_{0yy}^{\text{odd}} - i\tilde{t}_{12}\tilde{t}_{13}\mathcal{S}_{zxx}^{\text{odd}}\right)\Big]\lambda_{1,22}e^{-i\beta_{1,22}}.\end{aligned} \tag{C.34}$$

By summing equations (C.31)–(C.34) up, we obtain the odd-parity block of the jump operator in the setup of figure 3.

$$\tilde{K}_{\text{odd}} = \tilde{K}_{\text{odd}}^{11} + \tilde{K}_{\text{odd}}^{12} + \tilde{K}_{\text{odd}}^{21} + \tilde{K}_{\text{odd}}^{22}. \tag{C.35}$$

References

[1] Sato M and Fujimoto S 2009 *Phys. Rev.* B **79** 094504
[2] Oreg Y, Refael G and Von Oppen F 2010 *Phys. Rev. Lett.* **105** 177002
[3] Lutchyn R M, Sau J D and Das Sarma S 2010 *Phys. Rev. Lett.* **105** 077001
[4] Mourik V, Zuo K, Frolov S M, Plissard S, Bakkers E P and Kouwenhoven L P 2012 *Science* **336** 1003–7
[5] Rokhinson L P, Liu X and Furdyna J K 2012 *Nat. Phys.* **8** 795–9
[6] Das A, Ronen Y, Most Y, Oreg Y, Heiblum M and Shtrikman H 2012 *Nat. Phys.* **8** 887–95
[7] Deng M, Yu C, Huang G, Larsson M, Caroff P and Xu H 2012 *Nano Lett.* **12** 6414–9
[8] Churchill H, Fatemi V, Grove-Rasmussen K, Deng M, Caroff P, Xu H and Marcus C M 2013 *Phys. Rev.* B **87** 241401
[9] Finck A, Van Harlingen D, Mohseni P, Jung K and Li X 2013 *Phys. Rev. Lett.* **110** 126406
[10] Lutchyn R M, Bakkers E P, Kouwenhoven L P, Krogstrup P, Marcus C M and Oreg Y 2018 *Nat. Rev. Mater.* **3** 52–68
[11] Zhang H, Liu D E, Wimmer M and Kouwenhoven L P 2019 *Nat. Commun.* **10** 5128
[12] Prada E, San-Jose P, de Moor M W, Geresdi A, Lee E J, Klinovaja J, Loss D, Nygård J, Aguado R and Kouwenhoven L P 2020 *Nat. Rev. Phys.* **2** 575–94
[13] Pan H and Das Sarma S 2020 *Phys. Rev. Res.* **2** 013377
[14] Aghaee M *et al* 2023 *Phys. Rev.* B **107** 245423
[15] Choy T P, Edge J M, Akhmerov A R and Beenakker C W 2011 *Phys. Rev.* B **84** 195442
[16] Kjaergaard M, Wölms K and Flensberg K 2012 *Phys. Rev.* B **85** 020503
[17] Martin I and Morpurgo A F 2012 *Phys. Rev.* B **85** 144505
[18] Nadj-Perge S, Drozdov I K, Bernevig B A and Yazdani A 2013 *Phys. Rev.* B **88** 020407
[19] Pientka F, Glazman L I and Von Oppen F 2013 *Phys. Rev.* B **88** 155420
[20] Klinovaja J, Stano P, Yazdani A and Loss D 2013 *Phys. Rev. Lett.* **111** 186805
[21] Braunecker B and Simon P 2013 *Phys. Rev. Lett.* **111** 147202
[22] Vazifeh M and Franz M 2013 *Phys. Rev. Lett.* **111** 206802
[23] Nadj-Perge S, Drozdov I K, Li J, Chen H, Jeon S, Seo J, MacDonald A H, Bernevig B A and Yazdani A 2014 *Science* **346** 602–7
[24] Kim Y, Cheng M, Bauer B, Lutchyn R M and Das Sarma S 2014 *Phys. Rev.* B **90** 060401
[25] Pöyhönen K, Westström A, Röntynen J and Ojanen T 2014 *Phys. Rev.* B **89** 115109
[26] Peng Y, Pientka F, Glazman L I and Von Oppen F 2015 *Phys. Rev. Lett.* **114** 106801
[27] Ruby M, Pientka F, Peng Y, Von Oppen F, Heinrich B W and Franke K J 2015 *Phys. Rev. Lett.* **115** 197204
[28] Pawlak R, Kisiel M, Klinovaja J, Meier T, Kawai S, Glatzel T, Loss D and Meyer E 2016 *npj Quantum Inf.* **2** 1–5
[29] Feldman B E, Randeria M T, Li J, Jeon S, Xie Y, Wang Z, Drozdov I K, Andrei Bernevig B and Yazdani A 2017 *Nat. Phys.* **13** 286–91
[30] Jeon S, Xie Y, Li J, Wang Z, Bernevig B A and Yazdani A 2017 *Science* **358** 772–6
[31] Kim H, Palacio-Morales A, Posske T, Rózsa L, Palotás K, Szunyogh L, Thorwart M and Wiesendanger R 2018 *Sci. Adv.* **4** eaar5251
[32] Read N and Green D 2000 *Phys. Rev.* B **61** 10267
[33] Fu L and Kane C L 2008 *Phys. Rev. Lett.* **100** 096407
[34] Fu L and Kane C L 2009 *Phys. Rev.* B **79** 161408
[35] Hart S, Ren H, Wagner T, Leubner P, Mühlbauer M, Brüne C, Buhmann H, Molenkamp L W and Yacoby A 2014 *Nat. Phys.* **10** 638–43
[36] Pribiag V S, Beukman A J, Qu F, Cassidy M C, Charpentier C, Wegscheider W and Kouwenhoven L P 2015 *Nat. Nanotechnol.* **10** 593–7
[37] Moore G and Read N 1991 *Nucl. Phys.* B **360** 362–96
[38] Kitaev A 2006 *Ann. Phys., NY* **321** 2–111
[39] Nayak C, Simon S H, Stern A, Freedman M and Das Sarma S 2008 *Rev. Mod. Phys.* **80** 1083
[40] Hasan M Z and Kane C L 2010 *Rev. Mod. Phys.* **82** 3045
[41] Alicea J 2012 *Rep. Prog. Phys.* **75** 076501
[42] Beenakker C 2013 *Annu. Rev. Condens. Matter Phys.* **4** 113–36
[43] Das Sarma S, Freedman M and Nayak C 2015 *npj Quantum Inf.* **1** 1–13
[44] Aguado R 2017 *Riv. Nuovo Cim.* **40** 523–93
[45] Ivanov D A 2001 *Phys. Rev. Lett.* **86** 268
[46] Stern A and Lindner N H 2013 *Science* **339** 1179–84
[47] Stanescu T D and Tewari S 2013 *J. Phys.: Condens. Matter* **25** 233201
[48] Kitaev A Y 2001 *Phys.-Usp.* **44** 131
[49] Alicea J, Oreg Y, Refael G, Von Oppen F and Fisher M P 2011 *Nat. Phys.* **7** 412–7
[50] Zanardi P and Rasetti M 1999 *Phys. Lett.* A **264** 94–99
[51] Tanimura S, Nakahara M and Hayashi D 2005 *J. Math. Phys.* **46** 022101
[52] Zhang J, Devitt S J, You J and Nori F 2018 *Phys. Rev. A* **97** 022335
[53] Calzona A, Bauer N and Trauzettel B 2020 *SciPost Phys. Core* **3** 014
[54] Van Heck B, Akhmerov A, Hassler F, Burrello M and Beenakker C 2012 *New J. Phys.* **14** 035019
[55] Freedman M, Kitaev A, Larsen M and Wang Z 2003 *Bull. Am. Math. Soc.* **40** 31–38
[56] Wang Z 2010 *Topological Quantum Computation* vol 112 (American Mathematical Society)
[57] Aasen D *et al* 2016 *Phys. Rev.* X **6** 031016
[58] Plenio M and Huelga S 2002 *Phys. Rev. Lett.* **88** 197901
[59] Diehl S, Rico E, Baranov M A and Zoller P 2011 *Nat. Phys.* **7** 971–7
[60] Bardyn C E, Baranov M A, Kraus C V, Rico E, İmamoğlu A, Zoller P and Diehl S 2013 *New J. Phys.* **15** 085001
[61] Liu D E 2013 *Phys. Rev. Lett.* **111** 207003
[62] Zhang G and Baranger H U 2020 *Phys. Rev.* B **102** 035103
[63] Zhang G C 2020 *Phys. Rev.* B **102** 045111
[64] Lindblad G 1976 *Commun. Math. Phys.* **48** 119–30
[65] Lindblad C 2001 *Non-Equilibrium Entropy and Irreversibility* vol 5 (Springer)
[66] Breuer H P and Petruccione F 2002 *The Theory of Open Quantum Systems* (Oxford University Press)
[67] Weiss U 2012 *Quantum Dissipative Systems* (World Scientific)

[68] Gardiner C and Zoller P 2004 *Quantum Noise: a Handbook of Markovian and non-Markovian Quantum Stochastic Methods With Applications to Quantum Optics* (Springer)
[69] Santos R A, Iemini F, Kamenev A and Gefen Y 2020 *Nat. Commun.* **11** 5899
[70] Iemini F, Mazza L, Rossini D, Fazio R and Diehl S 2015 *Phys. Rev. Lett.* **115** 156402
[71] Iemini F, Rossini D, Fazio R, Diehl S and Mazza L 2016 *Phys. Rev.* B **93** 115113
[72] Touzard S *et al* 2018 *Phys. Rev.* X **8** 021005
[73] Geerlings K, Leghtas Z, Pop I M, Shankar S, Frunzio L, Schoelkopf R J, Mirrahimi M and Devoret M H 2013 *Phys. Rev. Lett.* **110** 120501
[74] Lu Y, Chakram S, Leung N, Earnest N, Naik R K, Huang Z, Groszkowski P, Kapit E, Koch J and Schuster D I 2017 *Phys. Rev. Lett.* **119** 150502
[75] Deng M, Vaitiekėnas S, Hansen E B, Danon J, Leijnse M, Flensberg K, Nygård J, Krogstrup P and Marcus C M 2016 *Science* **354** 1557–62
[76] Plugge S, Rasmussen A, Egger R and Flensberg K 2017 *New J. Phys.* **19** 012001
[77] Gau M, Egger R, Zazunov A and Gefen Y 2020 *Phys. Rev.* B **102** 134501
[78] Gau M, Egger R, Zazunov A and Gefen Y 2020 *Phys. Rev. Lett.* **125** 147701
[79] Verstraete F, Wolf M M and Ignacio Cirac J 2009 *Nat. Phys.* **5** 633–6
[80] Fujii K, Negoro M, Imoto N and Kitagawa M 2014 *Phys. Rev.* X **4** 041039
[81] Flensberg K 2011 *Phys. Rev. Lett.* **106** 090503
[82] Karzig T *et al* 2017 *Phys. Rev.* B **95** 235305